universität wien

DIPLOMARBEIT / DIPLOMA THESIS

Titel der Diplomarbeit / Title of the Diploma Thesis

„Increased Osteocyte Lacunae Density in Children with Osteogenesis Imperfecta Type I“

verfasst von / submitted by

Matthias Mähr

angestrebter akademischer Grad / in partial fulfilment of the requirements for the degree of

Magister der Pharmazie (Mag.pharm.)

Wien, 2022 / Vienna, 2022

Studienkennzahl lt. Studienblatt / degree programme code as it appears on the student record sheet:	UA 449
Studienrichtung lt. Studienblatt / degree programme as it appears on the student record sheet:	Diplomstudium Pharmazie
Betreut von / Supervisor:	Priv.-Doz. Dr. Nadja Fratzl-Zelman

Eidesstattliche Erklärung

Ich erkläre hiermit von Eides statt, dass ich die vorliegende Arbeit selbstständig und ohne Benutzung anderer als der angegebenen Hilfsmittel angefertigt habe. Die aus fremden Quellen direkt oder indirekt übernommenen Gedanken sind als solche kenntlich gemacht.

Die Arbeit wurde bisher in gleicher oder ähnlicher Form keiner anderen Prüfungsbehörde vorgelegt und auch noch nicht veröffentlicht.

Danksagung

An dieser Stelle möchte ich mich beim gesamten Team des LBIO bedanken.

Angefangen mit Sonja, Petra und Phaedra die mich mit viel Elan und Humor in die technischen Arbeiten im Labor eingeführt haben und mir auch bei der Arbeit am Elektronenmikroskop mit Rat und Tat zur Seite standen.
Dann möchte ich mich bei Priv. Doz. Dr. Markus Hartmann dafür bedanken, dass er mich für die Zeit meiner Diplomarbeit in seiner Forschungsgruppe aufgenommen hat und mir so die Möglichkeit gab den wissenschaftlichen Bereich näher kennenzulernen.
Auch Dr. Stephane Blouin, der mir stets bei diversen technischen Herausforderungen am Elektronenmikroskop zur Seite Stand und mir die von ihm entwickelte Methode näher brachte, bin ich sehr dankbar.
Weiters möchte ich mich sehr herzlich bei Prim. Priv. Doz. Dr. Jochen Zwerina dafür bedanken, dass er mir die Chance gegeben hat eine Zeit lang Teil des LBIO zu sein.
Und zu guter Letzt möchte ich mich noch ganz ausdrücklich bei meiner Betreuerin Priv. Doz. Dr. Nadja Fratzl-Zelman bedanken, die mir über die gesamte Dauer meiner Arbeit mit unermüdlichem Eifer zur Seite gestanden ist. Sei es in persönlichen Gesprächen, Telefonaten, Skype-Sessions oder per Email, Sie war stets erreichbar und hat mich im positiven Sinne gefordert und sehr gefördert. Ohne Ihre Unterstützung wäre diese Arbeit nicht möglich gewesen!

Abschließend möchte ich mich nochmal beim ganzen Team dafür bedanken, was Ihr für die OI Community und darüber hinaus leistet, ich weiß das sehr zu schätzen!

Table of contents

1. Introduction

Bones are the main component of the human skeleton and can be considered as rigid organs. They have multiple functions such as protection of internal organs, production of red and white blood cells (hematopoiesis), storage of minerals and furthermore have important endocrine functions. But their outstanding role is to provide mechanical support to the body and thus structure, shape and mobility. Due to their fascinating and complex macro, micro and nanostructure bones are lightweight, yet strong and hard, and at the same time though and not brittle (Wagermaier et al., 2015). They have a variety of shapes and sizes with the largest being the femur and the smallest being the stapes in the middle ear. Overall an adult has as many as 220 bones (Bartl, 2014). It is not hard to imagine that genetic alterations affecting bone metabolism will affect the individual at multiple levels. This thesis will focus on the effect on bone tissue of one of these conditions, called Osteogenesis imperfecta (OI). Here the skeleton becomes more fragile and is, depending on the severity of the disease, not able to fulfil all of its normal physiological functions, leaving people affected with great challenges in managing their lives (Rauch and Glorieux, 2004). Nevertheless, thanks to years of research, we now have a fundamental understanding of the underlying mechanisms that lead to the various forms of OI and consequently a whole string of possible treatments. Those involve pharmacological treatments, as well as, psychological support and very importantly, physical exercises (Rauch and Glorieux, 2004). As OI is an inherited, genetic disorder, the primary goal is not to heal this condition, but to treat symptoms effectively and to improve quality of life. The following pages will give an overview on the underlying causes of OI, the resulting symptoms and the alterations that occur on a material level. We will then focus on OI type I and on one specific bone cell, the osteocyte, as there is strong evidence of alterations in OI affecting these cells.

2. Background

2.1. Osteogenesis imperfecta

Osteogenesis imperfecta (OI) is a heritable, phenotypically and genetically very heterogeneous bone dysplasia. Also known as “brittle bone disease”, the primary clinical manifestation involves the skeleton with its hallmark features of low bone mass and increased bone fragility resulting in recurrent fractures, bone deformities and growth deficiency (Marini et al., 2017; Roschger et al., 2008). Beyond the strict skeletal manifestations, OI should be considered as a generalized connective tissue disorder with an array of associated secondary features, including blue sclera, hearing loss, dentinogenesis imperfecta, malocclusion, scoliosis, muscle weakness and ligamentous laxity (Forlino and Marini, 2016; Fratzl-Zelman et al., 2015; Roschger et al., 2008).

A reasonable estimate of the incidence of osteogenesis imperfecta is about 1 per 10000 individuals and is thus considered a rare disorder (van Dijk et al., 2011). About 90% of patients are heterozygous for mutations in the *COL1A1* or *COL1A2* genes coding for the α1- and α2-chains of type I collagen and there is no observed difference in the prevalence between sexes (Roschger et al., 2008). The inheritance is autosomal dominant and therefore one copy of the altered gene is sufficient to cause OI. That means there is a 50% chance for offspring to inherit the defect allele if one parent is affected (if both parents are affected the probability is 75%) and therefore to be a so-called positive carrier. It should be mentioned that we also see a high prevalence for de novo mutations (25 – 30%) where none of the parents are affected (Marini et al., 2017).

The mutations in *COL1A1* and *COL1A2* lead to alterations in the process of collagen synthesis and in bone cell metabolism. Collagen type I is the most abundant protein in the human body, making up to 30% of the body protein content and is the main component of the extracellular matrix of bone, skin, dentin, cornea, heart valves and aortic walls (Ricard-Blum, 2011).

As this disorder is phenotypically extremely heterogeneous, categorization of patients into separate types was shown to be useful to make prognosis and to find the appropriate therapeutic interventions (Fratzl-Zelman et al., 2015). In 1979 Sillence et al., proposed a classification into four types, based on clinical severity, ranging from mild to lethal (Van Dijk and Sillence, 2014). The most relevant characteristics of those four types of osteogenesis imperfecta are fracture rates, skeletal deformities and growth deficiency with clinical severity increasing from OI type I < type IV < type III < type II with the latter being perinatal lethal (Rauch and Glorieux, 2004; Van Dijk and Sillence, 2014).

OI Type	Inheritance	Features
I	AD	Osseous fragility (variable) Adulthood hearing loss Blue sclerae
II	AD, AR	Extremely severe osseous fragility Perinatally lethal
III	AR	Moderate to severe osseous fragility Normal sclerae Severe deformity of long bones and spine Variable clinical and radiographic phenotypes
IV	AD, AR	Osseous fragility Generally normal sclerae Severe deformity of long bones and spine

AD = autosomal dominant; AR = autosomal recessive; OI = osteogenesis imperfecta

Figure 1: *1979 Sillence classification of osteogenesis imperfecta. Detailed features of the various types are given in the right column (Van Dijk and Sillence, 2014). Classifying OI into clinical types helps physicians make more accurate prognosis and decide on the appropriate treatment. The Sillence classification has been extended continuously in recent years to 18 different types. These new types are mostly autosomal recessive (AR) and are associated with defects in non-collagenous genes. The first type of OI that has been described with no mutation in a collagen gene was OI type V (Glorieux et al., 2000).*

In the years 2000 to 2002, Francis H. Glorieux and Frank Rauch described phenotypically three additional types (V, VI, and VII) with no underlying collagen-gene mutations, adding complexity to this heterogeneous dysplasia. This resulted in further investigation of genes being responsible for the different forms of OI (Glorieux et al., 2000; Glorieux et al., 2002; Ward et al., 2002).

Since 2006, when a defect in the Cartilage Associated Protein (*CRTAP*) was identified as the underlying cause of OI type VII, novel mutations in collagen-related genes have been found to cause these new forms of the disease, which has led to a further expansion of the original classification system to actually XVIII types of OI (Fratzl-Zelman et al., 2015; Jovanovic et al., 2021). It is now well accepted that OI is also caused by "a wide variety of genes encoding proteins involved in type I collagen synthesis, processing, secretion and post-translational modification, as well as in proteins that regulate the differentiation and activity of bone-forming cells" and further mineralization of the extracellular matrix (Marini et al., 2017). Although mutations in those genes only account for 10-15% of all OI cases, they underscore the fact that OI is predominantly a collagen-related disorder (Forlino and Marini, 2016). This thesis will focus on OI type I, which accounts for 80–90% of all OI cases and which is caused by structural or quantitative mutations in the collagen genes themselves (Roschger et al., 2019).

A point mutation affecting a glycine residue in either *COL1A1* or *COL1A2* is the most common sequence abnormality associated with OI (Roschger et al., 2008). Such a defect

results in the production of a mixture of normal and structurally abnormal collagen type I, which in turn results in a clinical phenotype that varies from mild to lethal depending on which α-chain is affected. Glycine substitutions in the α1 helical domains lead to more severe phenotypes (including lethality), whereas less severe forms like type I are associated with mutations in the α2 helical domain. These types of mutations that alters the amino acid sequence of the secreted α1 or α2-collagen chains and therefore the structure of collagen are designated as qualitative mutations. In contrast, mild forms of OI are generally related to haploinsufficiency of the α1-collagen chain, leading to decreased production of structurally normal collagen type I (Forlino and Marini, 2016; Fratzl-Zelman et al., 2015; Marini et al., 2017; Rauch and Glorieux, 2004). These mutations are called quantitative mutations (Tauer et al., 2021).

As the collagen protein plays such a central role in OI, we will now focus on it more closely and explain structure, synthesis and folding of collagen molecules.

2.2. Collagen type I

As mentioned above, collagen type I is the most abundant protein in the human body and is particularly important for bone. Collagen type I molecules consist of three polypeptide chains (two α1- and one α2-chains), which form a triple helical structure (Roschger et al., 2008). The triple helical sequences comprised of repeated Gly-Xaa-Yaa sequences, with Xaa and Yaa usually being proline and 4-hydroxy-proline. Glycine (Gly) represents the most abundant amino acid in the collagen protein and plays a crucial role for the physiological function of collagen (see below) (Ricard-Blum, 2011). The *COL1A1* gene codes for the two pro-α1-chains and the *COL1A2* gene for the pro-α2-chain and together they form the type I pro-collagen molecule. The biosynthesis of type I pro-collagen is, despite its simple structure, extremely complicated involving multiple steps inside and outside the cell and an array of proteins for post-translational modifications (Marini et al., 2017). The first step is the transcription of the *COL1A1* and *COL1A2* genes in the nucleus. Next the mRNA moves into the cytoplasm where it interacts with ribosomes. After translation into the rough endoplasmic reticulum (ER) it is now ready for post-translational modification. At this stage, the molecule is referred to as pre-pro-collagen. There are three major modifications that take place in order for the molecule to become pro-collagen. First the signal peptide on the N-terminus has to be removed. Next multiple lysine and proline residues get hydroxylated mostly via prolyl-3-hydroxylase 1, prolyl-4-hydroxylase and lysyl-hydroxylase. In the final step of the process these hydroxyl groups get glycosylated with galactose and glucose. The hydroxylated and glycosylated chains are now ready to assemble and twist into a triple helix (Baum and Brodsky, 1999; Malhotra and Erlmann, 2015). The resulting pro-collagen molecule consisting of a helical and two globular parts at both ends, is transported to the

Golgi apparatus where final modifications take place before it is secreted by exocytosis. Once secreted, they are being again processed by enzymes called collagen peptidases who cleave and remove the N- and C- globular ends of the pro-collagen molecule. The now called tropocollagen is then covalently bonded to other tropocollagen molecules via lysyl-oxidase to form a so-called collagen fibril. Numerous collagen fibrils can then be assembled into collagen fibers (Ricard-Blum, 2011; Viguet-Carrin et al., 2006).

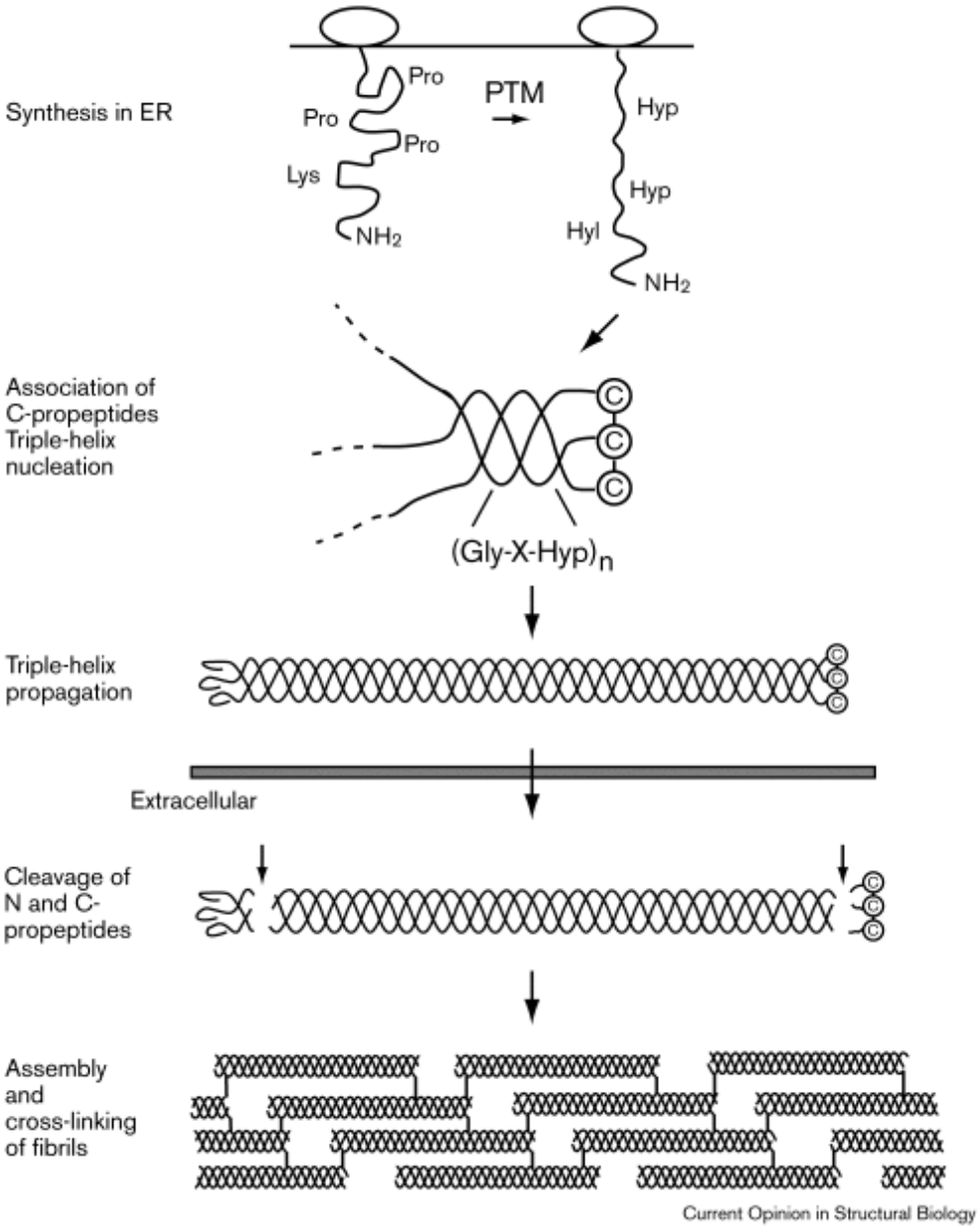

Figure 2: *Synthesis and folding of collagen (Baum and Brodsky, 1999). Production of collagen type I is extremely complex and involves multiple steps inside and outside of the cell (Marini et al., 2017). Mutations in collagen genes but also in genes coding for proteins that are involved in post-translational collagen modifications have severe adverse effects for affected people.*

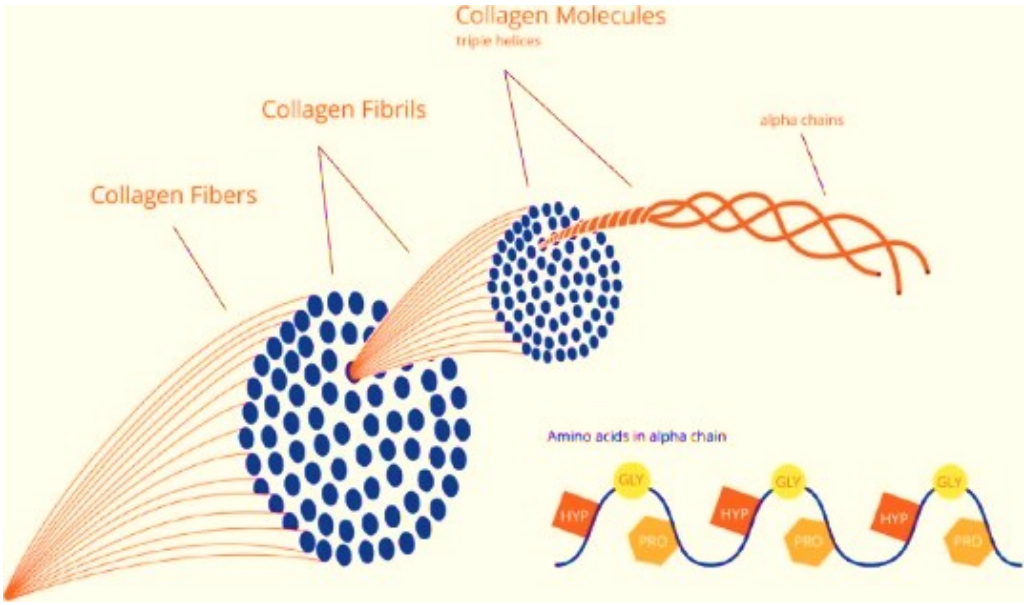

Figure 3: *Several collagen fibrils assemble into collagen fibers (Nijhuis et al., 2019). These collagen fibers are the main component of the extracellular matrix of bone, skin, dentin, cornea, heart valves and aortic walls (Roschger et al., 2008). Glycine, proline and 4-hydroxy-proline are the main amino acids of the collagen type I α chains.*

But what is the reason for the crucial role of glycine in collagen proteins? First of all, it is important to know that glycine is the smallest of all amino acids and has no side chain. Due to the very tight packing of the collagen protein, glycine is the perfect amino acid to fit within the helix. There is simply not enough space in the center for a larger side group than the single hydrogen atom. That is also the reason why proline and hydroxy-proline rings must point outward. Second of all, as mentioned above, we find glycine at every third position which makes it the most abundant amino acid in collagen. Mutations affecting glycine residues, mostly substitutions by bulkier and more polar groups have therefore severe consequences for the correct folding and the stability of the collagen protein. Proline and hydroxyl-proline also play a crucial role in stabilizing the triple helix but overall glycine is the key factor for the steric integrity of the collagen protein (Bella, 2016; Ricard-Blum, 2011; Viguet-Carrin et al., 2006).

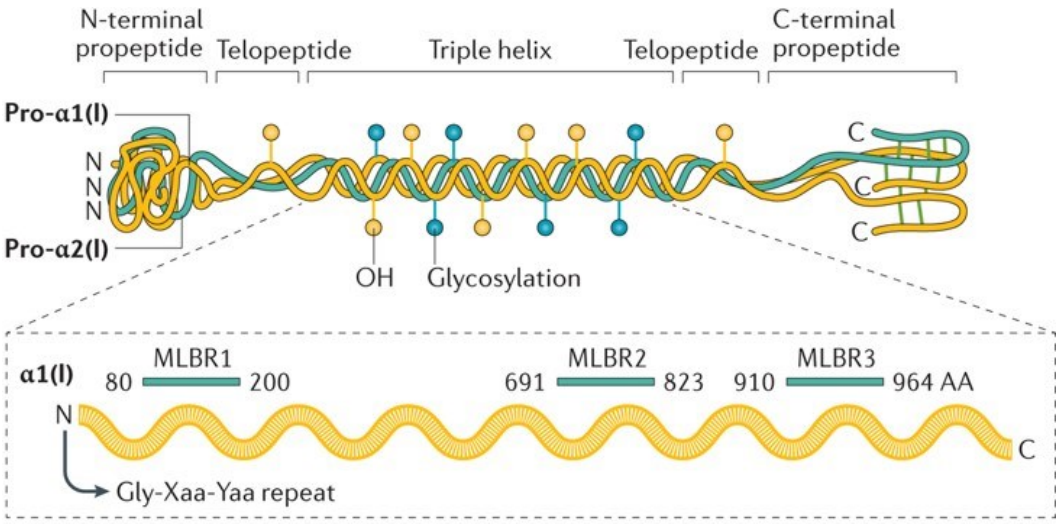

Figure 4: *Structure of collagen (Marini et al., 2017). The triple helical sequences comprise repeated Gly-Xaa-Yaa sequences, with Xaa and Yaa being proline and 4-hydroxy-proline. As glycine is the smallest amino acid with no side chains, it allows the extremely tight packing of the triple helix. Pre-pro-collagen undergoes extensive hydroxylation and glycosylation.*

2.3. Bone characteristics in OI

Research on human bone can be performed on undecalcified, plastic embedded bone biopsy samples, which can for example be obtained from the iliac crest of patients. Bone histomorphometry represents a standardized method, where 3-5µm thick sections from these samples are stained, generally by Goldner´s trichrome and analyzed by light microscopy to evaluate bone structure, cell number and activity (Rauch, 2006).

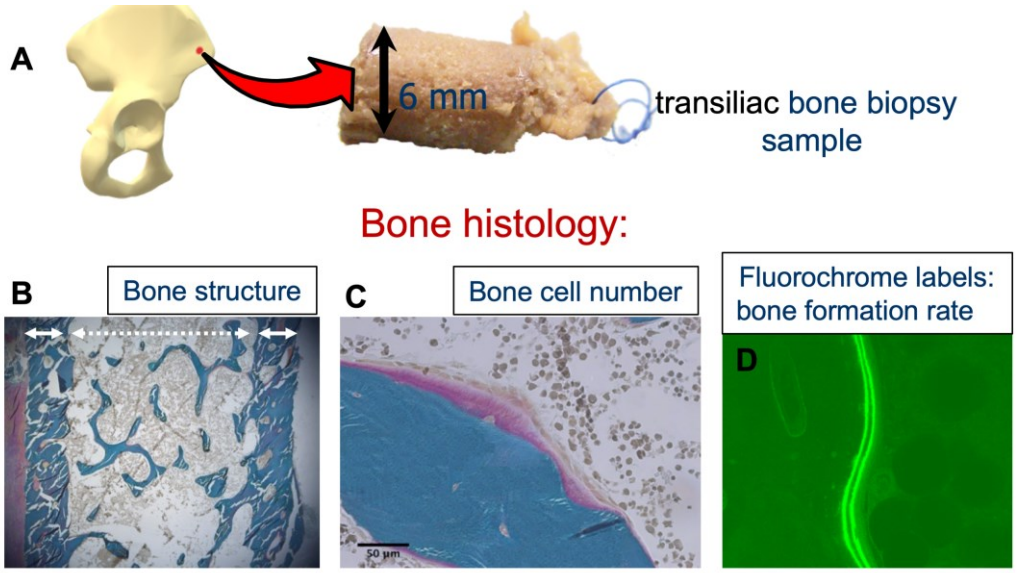

Figure 5: *A) Picture of a transiliac bone biopsy sample. B) 3,5µm thick sections from the sample are used to study bone structure. C) Stained sections can be analyzed by light microscopy to study bone cells. D) By using fluorochrome labels, bone formation rate can be examined (Mahr et al., 2021).*

In 2000, Glorieux et al. established a pediatric reference cohort for bone histomorphometry based on iliac bone samples from 58 healthy individuals, aged between 1.5 and 22.9 years. As tetracycline labeling was performed in 48 subjects prior to the procedure, these biopsy samples provide static and dynamic bone formation data. Doing that, they established normative data for iliac bone histomorphometry in growing children spanning the whole growth period (Glorieux et al., 2000).

Within the same year Rauch et al. presented an article where they compared bone histomorphometry parameters from children with OI with that reference cohort. The OI cohort consisted of tetracycline-labeled iliac bone biopsy samples from 70 children with different forms of OI caused by collagen-gene mutations. 32 of those samples where from children with OI type I (Rauch et al., 2000). For this thesis we reevaluated 19 of those 32 samples together with 24 age matched controls from the reference cohort (see below).

Bone histomorphometry revealed that children with OI have thinner cortices and decreased trabecular thickness and trabecular number, which is consistent with the general picture of decreased bone mass in OI compared to healthy individuals (Glorieux et al., 2000; Rauch et al., 2000). Figure 5 shows a bone histomorphometry section compared to sections from OI type I, III and IV biopsy samples. The low bone mass is evident in all three types even if to a lesser extent in OI type I when compared to type III and IV.

Rauch et al., further showed significantly increased trabecular surface-based bone formation indices like osteoblast surface per bone surface (Ob.S/BS) in all three forms of OI. This indicates that there are more osteoblasts in OI than in healthy bones. However, mineral apposition rate (MAR) was decreased in OI. Consequently, bone formation rate (BFR), when related to osteoblast surface, was lower than in healthy controls (Roschger et al., 2008). The authors concluded that patients with OI have more osteoblasts, but they build less bone than expected because the matrix production at the single cell level is decreased (Rauch et al., 2000). Furthermore, they did not only find alterations concerning osteoblasts but also osteoclasts, as osteoclast surface per bone surface (Oc.S/BS) was higher in OI than in the control group indicating all together high bone remodeling activity in OI bone (Fratzl-Zelman et al., 2009).

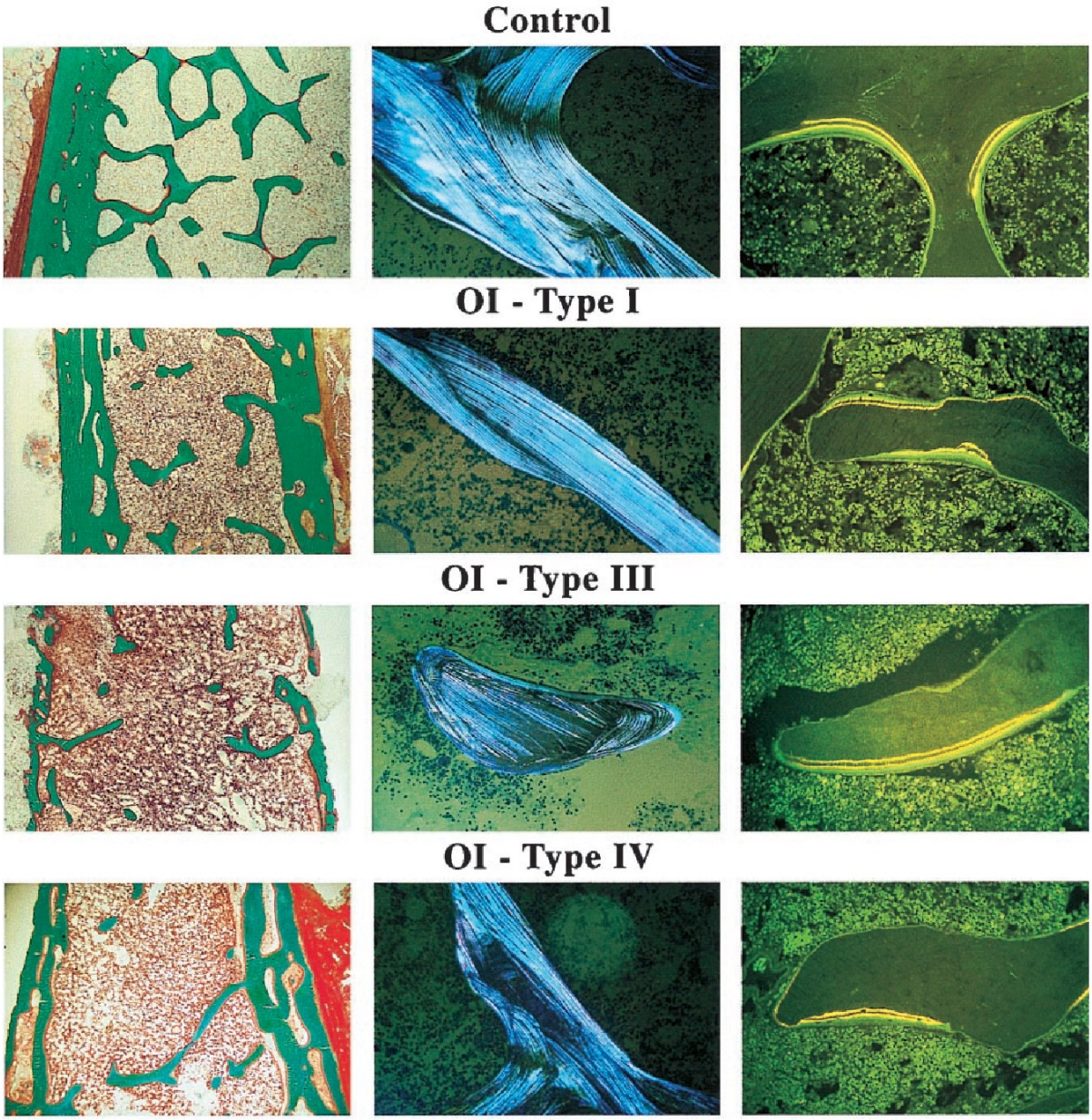

Figure 6: *Bone histomorphometry sections of biopsies from a control subject and OI patients (Rauch et al., 2000). OI iliac bone samples show thinner cortices, less trabecular thickness, less trabecular number and a decreased core width. The middle column shows thinner lamellae in OI that seem less smooth than in the control subject. In the right column, tetracycline labels under fluorescent light do not reveal disturbances in the process of mineralization.*

Apart from alterations in OI related to bone mass and bone cells there are also major alterations on the material level. A typical abnormality in OI bone is the higher degree of mineralization of the bone matrix.

In 1999 Boyde et al., analyzed bone matrix mineralization in transiliac bone biopsy samples from children with OI by backscattered electron imaging using a backscattered electron microscope (Boyde et al., 1999; Jones et al., 1999). They found the mineralization density to be higher in OI samples than in healthy controls. They assumed that hypermineralization is related to the underlying mutations and therefore to the severity of OI. Thus, they thought

the more severe the type the more mineralized the matrix. This assumption was later challenged by Weber et al. in 2006 who did not find any differences in matrix mineralization density between different types of OI severity (Weber et al., 2006). In 2008 Roschger et al., compared bone matrix mineralization in bone biopsy samples from children with quantitative and mild forms of qualitative mutations (thus, all clinically classified as OI type I) and showed that hypermineralization was not dependent on different collagen mutations. Therefore, hypermineralization of the bone matrix is now considered as a key characteristic of OI bone independently of clinical severity and type of mutation (Fratzl-Zelman et al., 2015). The higher mineral content contributes to stiffer bones, which combined with the net deficit in bone quantity plays a crucial role in the bone brittleness and fragility. At present it is still unclear what are the mechanisms leading to increased mineralization density. One possibility is that the mineralization kinetics, i.e. the time course of mineral accumulation within a newly formed unmineralized matrix or osteoid, is altered in OI, which might indicate a failure in the osteoblast differentiation pathway. This could lead to an altered synthesis of non-collagenous matrix proteins and proteoglycans, and consequently to disturbances in bone matrix stoichiometry (Roschger et al., 2008; Vetter et al., 1991). All these studies also show that bone biopsy samples are a very useful tool to study cellular and bone material properties in healthy and diseased bone (Mahr et al., 2021) (For more information see supplementary material A).

2.4. Osteogenesis imperfecta type I

As afore mentioned, Osteogenesis imperfecta type I represents the mildest form of OI, being also the most common type with an incidence of around 1 in 30 000 individuals (van Dijk et al., 2011). As there are no major bone deformities, this form is designated a non-deforming type. OI type I is often characterized by blue sclera, increased vertebral fractures and mild forms of scoliosis. Body height and weight are usually normal, or slightly reduced, which leads to body mass indices (BMI) that are similar to those of people without OI (Graff and Syczewska, 2017). Furthermore, a slight deficit in muscle strength in children and adolescents with OI type I is observed, which is nonetheless still compatible with relatively normal muscle function and performance (Veilleux et al., 2014). Related to those findings, another clinical characteristic is the association between OI and joint hypermobility due to ligamentous laxity, resulting in an increased risk of joint injuries (Arponen et al., 2014). Apart from frequent fractures, people with OI type I are usually not adversely affected in their everyday activities and apart from a few restrictions, are able to live a normal and active life.

As stated above, OI type I is caused by different types of mutations. Qualitative mutations are usually point mutations that affect at 85% a substitution of a glycine residue in *COL1A1*

or *COL1A2*, which results in the production of a mixture of normal and structural abnormal collagen. Such structural collagen defects can result in either mild, severe or lethal forms of OI. Quantitative mutations are usually nonsense or frameshift mutations in *COL1A1*. This results in unstable transcription products of the affected gene which are then destroyed by a process called nonsense-mediated decay (Byers, 2002; Roschger et al., 2008). As there is still an intact *COL1A1* allele, α1-chains with a normal amino acid sequence are also produced. Consequently, the overall collagen synthesis is reduced by 50%. This type of mutation nearly always results in a clinically mild form of OI (Roschger et al., 2008). As described by Roschger et al., in 2008 OI type I caused either by qualitative or quantitative mutations show a similar decrease in bone mass, reduced trabecular number and thickness, and decreased cortical width (see Figure 6) (Roschger et al., 2008).

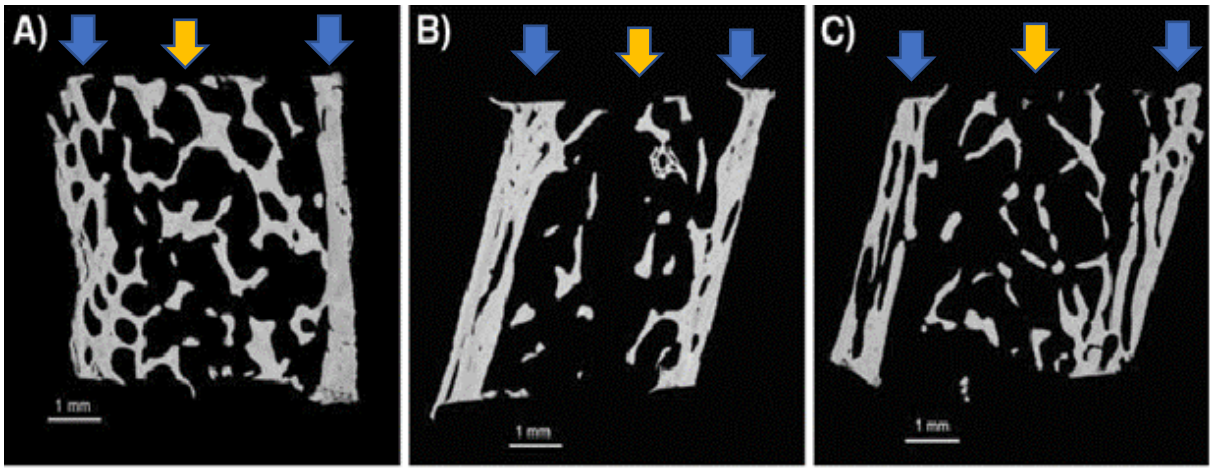

Figure 7: *Back-scattered electron microscopy images of transiliac bone biopsy samples showing typical structural OI type I characteristics: fewer number of trabeculae and decrease in trabecular thickness and thinner or more porous cortices. A) Healthy control B) OI-I (quantitative mutation) B) OI-I (qualitative mutation). Blue arrows show cortices and yellow arrows show trabeculae. (Roschger et al., 2008)*

Moreover, by applying quantitative back-scattered electron imaging (qBEI), they found a significantly higher mineral content in OI bone than in the control group, which is in line with findings by Boyde et al., in 1999 and Weber et al., in 2006. Interestingly, the degree of mineralization of the bone matrix of children with qualitative mutations was similar to the ones with quantitative. Thus the abnormal mineralization was not dependent on the underlying mutation (Roschger et al., 2008). Later on in other studies, hypermineralization was also shown in several new forms of OI without any collagen-gene mutations, as well as in OI mice models (Marini et al., 2017). Therefore, it seems very likely that other factors than the collagen structure itself are responsible for the over-mineralization in OI bone (Roschger et al., 2008).

To gain further insight into the abnormal mineralization in OI, Fratzl-Zelman et al., reevaluated in 2014 the biopsy samples from the OI type I group and the reference cohort by small-angle X ray scattering (SAXS). They found a similar crystal size in bone of healthy children and in the OI group. Thus, it was concluded that size and shape of the hydroxyapatite crystals are not affected by the collagen alterations in OI, but the density of mineral particles is increased by about 12% in OI bone (Fratzl-Zelman et al., 2014). As previously observed for bone matrix mineralization, there was again no difference in mineral particle size between qualitative and quantitative mutations. The authors therefore concluded that the increased mineral content in OI bone is due to higher density of mineral particles, which might be due to impaired osteoblastic function rather than to altered structure of the collagen matrix (Fratzl-Zelman et al., 2014). This assumption is in line with the already discussed hypothesis of altered early mineralization process in OI presented by Roschger et al., in 2008 (Roschger et al., 2008).

2.5. Aim of the study

Findings of Rauch et al., in 2000, Roschger et al., in 2008 and Fratzl-Zelman et al., in 2014 point in the direction of impaired osteoblastic function. In summary: bone histomorphometry showed that osteoblasts in OI produce only half the amount of matrix, even though there are more osteoblasts present. qBEI measurements showed that independently of specific collagen mutations, the bone matrix is hypermineralized. And finally, the combination of synchrotron SAXS with qBEI showed more densely packed mineral particles and again no difference between the two forms of mutations in OI type I. Furthermore, impaired osteoblast differentiation, abnormal cell metabolism and altered secretion of non-collagenous proteins were observed in OI (Vetter et al., 1991). Together, these findings suggest severely impaired osteoblastic function and a bone cell defect downstream of the collagen mutation might be responsible for bone abnormalities in OI. In accordance, it has been reported that not only osteoblasts are dysfunctional in OI but also osteocytes, the cells embedded within the mineralized matrix and offspring of osteoblasts (Bonewald, 2011; Zimmerman et al., 2019). Indeed, in 2000, when Rauch et al., investigated bone histomorphometry, they reported an elevated number of osteocytes in OI but this was not quantified at that time (Rauch et al., 2000). Later on, in 2015 Imbert et al., again observed increased osteocyte density in OI bone and this time that observation was quantified by counting the number of osteocyte lacunae. They found a 50% increase in osteocyte lacunae density compared to healthy controls (Imbert et al., 2015). In 2017 the spotlight was once again put on osteocytes in OI when Blouin et al investigated osteocyte lacunae in OI type V bone (Blouin et al., 2017). OI type V is a very special form of OI and not per se comparable to OI type I. It was the first type where no mutation in a collagen type I encoding gene could

be found. Further it is characterized by hyperplastic callus formation after fractures and a severely altered bone lamellation that results in a “mesh-like” appearance of the bone tissue. By establishing five parameters describing number, size and shape of the lacunae they paved the way for detailed analysis of osteocytes. They found significantly increased lacunae density in type V OI bone. The highly unorganized bone lamellation together with the increased osteocyte lacunae density indicate an exuberant primary and woven bone formation in OI type V. These findings underline the assumption of impaired osteocyte function in OI (Blouin et al., 2017).

Because, both studies are limited to few patients we aimed to characterize osteocyte lacunae characteristics in a larger cohort of children with OI type I and healthy children of similar age. Therefore, we reanalyzed the bone biopsy samples from the pediatric control cohort from Glorieux et al., and the OI type I group established by Rauch et al in 2000, by quantitative backscattered electron imaging at a nominal resolution of 0.9 µm per pixel (Glorieux et al., 2000; Rauch et al., 2000). By using the parameters established by Blouin et al., we evaluated number, size and shape of the lacunae to gain further insights into osteocyte characteristics and bone metabolism in OI (Blouin et al., 2017).

In order to shed more light on the osteocyte and why this cell is thought to play an essential role in bone homeostasis, the next paragraph will focus on the fascinating osteocyte biology, before we describe the applied method and present the results of the study.

3. Osteocytes: State of the art

3.1. Master orchestrators of bone metabolism

There are three types of cells that direct bone metabolism. There is the osteoblast who builds the collagenous matrix, there is the osteoclast who resorbs bone and then there is the osteocyte who acts as a master orchestrator of bone metabolism and directs mineralization (Bonewald, 2011). Osteocytes are by far the most numerous bone cell and represent up to 90 to 95% of all bone cells. In the adult human skeleton the total number of osteocytes is estimated to be around 42 billion (Buenzli and Sims, 2015). With an average half-life of around 25 years they are furthermore the longest living ones (Bonewald, 2011).

It was long thought that the most important actions in bone metabolism take place on the bone surface. Consequently, the cells that got all the attention were osteoblasts and osteoclasts and therapeutics were primarily developed to target those two cell types. Nevertheless in recent years the central role of osteocytes in bone metabolism and their function beyond bones has gradually been revealed (Bonewald, 2011).

3.2. Osteocytogenesis

As already mentioned, osteocytes are descendants of mature matrix-producing osteoblasts. Besides becoming osteocytes, osteoblasts can also become lining cells or undergo programmed cell death (apoptosis) (Robling and Bonewald, 2020). The mechanisms deciding on the fate of an osteoblast are currently poorly understood. What we know is that in order to differentiate into an osteocyte, the former osteoblast becomes surrounded by unmineralized matrix, the osteoid and later on by mineralized matrix (Dallas and Bonewald, 2010). It was long thought that this happens by passive entrapment but there is growing evidence that the process of osteocytogenesis is highly regulated at the cell level. For example by active migration of osteoblasts into osteoid, accompanied by a decrease of collagen synthesis and an upregulated expression of matrix metalloproteinases which can cleavage collagen (Chen et al., 2018; Robling and Bonewald, 2020). In the following paragraphs we will briefly discuss the theories behind passive entrapment. Afterwards we will focus more closely on the process of active migration and explain why this theory is more relevant today.

3.2.1. Passive entrapment

Passive entrapment of osteocytes was thought to occur during bone formation when mature osteoblasts get gradually embedded within the surrounding unmineralized extracellular matrix (osteoid) and neighbor osteoblasts secrete osteoid on top of the embedding cell (Bonewald, 2011; Chen et al., 2018). This process is accompanied by a striking change of cell morphology as the initially polygonal shaped cell starts to form cellular extensions toward the mineralizing front. Simultaneously the preosteocytes (also called osteoid-osteocytes) start to shrink and to take on a more ellipsoid shape (Dallas and Bonewald, 2010). The transformation of the cell morphology continuous as the cellular extensions evolve into dendritic processes that start to extend toward either the vascular space or the bone surface (Bonewald, 2011). The dendrites continuously extend, form connections with previously embedded cells and thereby get anchored into the osteocyte network. The tunnels formed by the extension of the dendrites are called canaliculi. The preosteocyte now begins the mineralization process surrounding itself with hydroxyapatite and thereby forming a cave called lacuna. When the osteoid surrounding the cell is fully mineralized and the change in cell morphology is completed, the preosteocyte is referred as a mature osteocyte, that is now functionally part of the osteocyte lacunocanalicular network (Chen et al., 2018). Interestingly, a recent study shows a lowly mineralized region around canaliculi in the transition zone between mineralized matrix and osteoid. This is a further proof that osteocytes play a crucial role at the early stages of mineralization (Ayoubi et al., 2021).

3.2.2. Active migration

As mentioned above, recent findings indicate an active role of osteoblasts and a more active and invasive role of osteoid-osteocytes (preosteocyte) in the process of osteocytogenesis. It is very unlikely that such striking changes in morphology and gene expression are merely due to passive entrapment (Bonewald, 2011). In fact, it became evident within the last years that the process of osteocytogenesis is accompanied by active matrix remodeling mediated by different matrix metalloproteinases (MPP) secreted by osteocytes. For example, along the dendritic processes, collagen fibrils are actively cleaved by a specific, cell membrane-bound collagenase (MT1-MMP/MMP14). In 2005 Holmbeck et al. showed that MMP14 null mice are not able to develop a functional canalicular system, due to reduced number and length of dendritic processes (Holmbeck et al., 2005). This observation strongly speaks against any passiveness during that development. There are also genes that are only transiently expressed during that transition like E11/gp33. E11 is localized at nascent dendritic processes that start stretching into the bone matrix. Upon osteocyte maturation the E11 expression stops but interestingly is upregulated again in response to mechanical loading (Schulze et al., 1999; Zhang et al., 2006). Again, deletion of that gene resulted in

decreased canaliculi formation in vivo (Staines et al., 2017). Finally it was also observed that osteoblasts migrate into the osteoid-like dense collagen matrices over a large distance, accompanied by the already mentioned change in protein expression and cell shape (Chen et al., 2018; Robin et al., 2016).

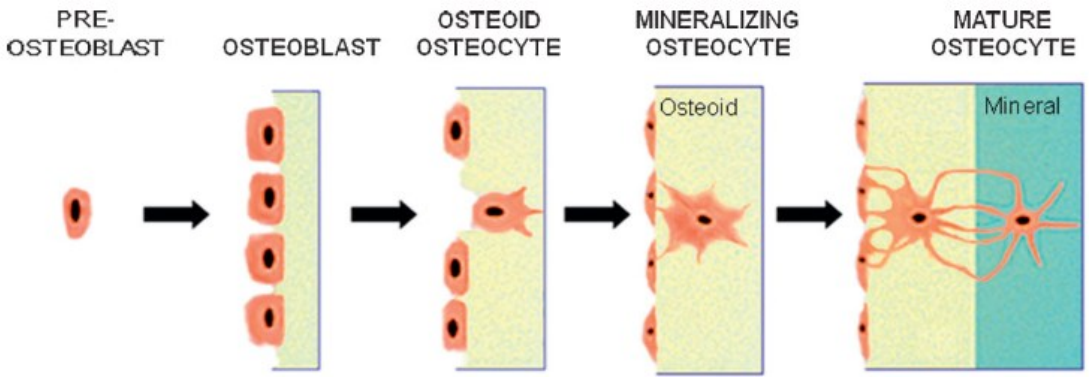

Figure 8: *Phases of osteocytogenesis from a pre-osteoblast to a mature osteocyte (Bonewald, 2011). This process is accompanied by major changes in cell morphology like becoming more ellipsoid and forming long dendritic processes.*

To summarize, the osteocyte is a star shaped cell with a single nucleus that resides in spaces called lacunae inside the mineralized bone matrix. They form a tremendous network of long cytoplasmic extensions, occupying tiny canals called canaliculi. It is estimated that the total length of all osteocytic processes connected end-to-end adds up to 175,000 km (Buenzli et al., 2018; Buenzli and Sims, 2015). Thanks to these dendritic processes osteocytes are connected to each other and are thereby able to communicate and exchange nutrients through gap junctions (Knothe Tate et al., 2004). Furthermore they are connected to the bone surface, the bone marrow and blood vessels (Robling and Bonewald, 2020). Osteocyte lacunae and canaliculi form together a functional network, the lacunocanalicular system.

3.3. Osteocyte functions

As mentioned at the beginning of this chapter, osteocytes were long thought to be static cells that get passively embedded inside the bone matrix. Therefore, they did not get much attention until the focus of bone research shifted towards them 15 years ago. The main problem in performing research on osteocytes, is their extremely hard accessibility as they are embedded within the mineralized matrix (Franz-Odendaal et al., 2006; Robling and Bonewald, 2020). This is also why osteoblasts and osteoclasts are much better investigated as they are located on the bone surface. But new generations of osteocyte cell lines, new techniques of identifying osteocyte markers and new ways of imaging osteocytes with electronic microscopes helped to gradually reveal their functions and show their importance in bone metabolism and beyond (Bonewald, 2011).

As mentioned earlier osteocytes reside in spaces called lacunae and form dendritic processes that run through canaliculi. The cell and the dendrites are separated from the mineralized matrix by the so-called pericanalicular space filled with fluid which exposes them to sheer stress.

There are 5 major physiological functions of osteocytes:

- Remodeling of the surrounding bone matrix
- Mechanosensing
- Regulation of osteoclasts
- Regulation of osteoblasts
- Communication with distant organs (endocrine function)

3.3.1. Remodeling of the surrounding matrix (osteocyte-osteolysis)

Osteocytes are able to remove and replace their perilacunar and pericanalicular matrix under calcium-demanding conditions. Due to the vast number of osteocytes in human skeleton, the ability of osteocytes to release calcium from their perilacunocanalicular matrix can have a significant effect on serum calcium levels (Robling and Bonewald, 2020). It was shown that lactating mice have larger osteocyte lacunae in their long bones and vertebrae than virgin mice (Qing et al., 2012; Robling and Bonewald, 2020). This ability of osteocytes to remove matrix is enabled by expression of genes normally associated with osteoclasts, like cathepsin K and TRAP. Additionally, the lacunocanalicular system shows a decreased pH within its network during osteocytic osteolysis. Therefore osteocytes have to become more resistant to acidification of their extracellular environment during such times (Jahn et al., 2017).

Besides these physiological processes during calcium demanding periods, pathologic removal of the perilacunocanalicular matrix can also occur in diseases like hyperparathyroidism, hypophosphatemic rickets and osteoporosis (Tsourdi et al., 2018).

3.3.2. Mechanosensing

One function that has been known for a long time is that of mechanosensation. Thanks to their distribution throughout cortical and trabecular bone, the vast network they build and their complex connections to each other, they are perfectly fitted to sense mechanical loading or the lack of it (Bonewald, 2011).

In order to be mechanosensitive, osteocytes express a diverse range of proteins to sense mechanical changes of the environment. For example, integrin complexes and ion channels are considered important mechanosensors of the cells but also gap-junctions play an important role as they help osteocytes to communicate with each other. Interestingly the cell processes seem to be more mechanosensitive than the cell body itself (Robling and Bonewald, 2020). There have been put forward a number of possible physical stimuli to which osteocytes respond. One very likely mechanism is fluid flow through the lacunocanalicular system. Loading and therefore bending of the bone induces movements in the fluid which in turn induces shear stress on the cell membrane. Osteocytes sense these pressure gradients and react by putting forward corresponding signals to cells on the bone surface (Qin et al., 2020; Robling and Bonewald, 2020).

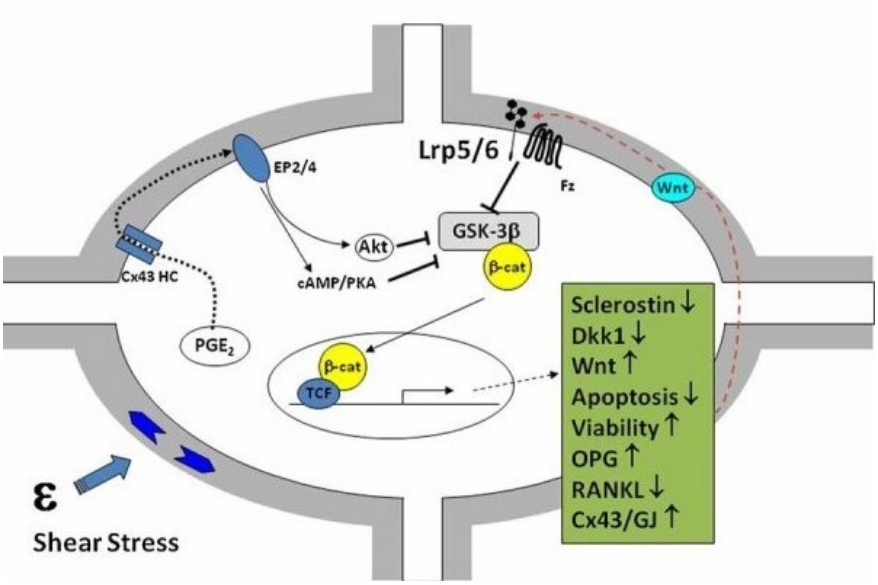

***Figure 9**: Osteocytes sense shear stress on their cell membrane and react by increasing transcription of certain genes and increasing or decreasing the secretion of certain factors. For example by downregulating the secretion of Sclerostin and RANKL they inhibit bone resorption and by upregulating OPG secretion they promote bone formation (Bonewald, 2011; Robling and Bonewald, 2020).*

The osteocytic ability for mechanosensing and mechanotransduction is the reason why bones are able to adapt to external loading conditions. This is also exactly why physical exercise is so important in order to maintain strong and healthy bones. Even in patients with severe forms of OI, multiple studies have shown that physiotherapy can improve the wellbeing of affected persons (Marr et al., 2017; Mueller et al., 2018). But not only people with OI benefit from regular deliberate training. As the population gets older and moreover because osteocytes are known to die with ageing and with age-related disorders like osteoporosis, the importance of lifelong activity cannot be emphasized enough. And that includes physical exercise (Bonewald, 2019; Bonewald, 2017; Milovanovic et al., 2015).

3.3.3. Regulation of osteoclasts

Osteoclasts are the main players when it comes to bone resorption and are therefore crucial for maintaining, repairing and remodeling of bones. By secreting acid, collagenases and cathepsin K they are able to break down mineralized and unmineralized bone matrix which additionally helps regulate the level of blood calcium. Active, bone resorbing osteoclasts are exclusively located in so called resorption lacunae on the bone surface. Osteoclastogenesis is triggered by hormones and factors like parathyroid hormone (PTH), calcitonin, Receptor activator of nuclear factor kappa-B ligand (RANKL) and osteoprotegerin (OPG). As we learned osteocytes are connected to the bone surface and

therefore also to osteoclasts. One way to coordinate osteoclast activity is by controlling the RANKL/OPG mechanism (Wang and McCauley, 2011).

RANKL is a protein that binds the RANK receptor on cells of the myeloid lineage like osteoclasts and plays a vital role in the bone remodeling process. Among other things it is essential for osteoclastogenesis and osteoclast differentiation and is therefore one of the key factors of bone resorption. It has been shown within the last years that osteocytes and not osteoblasts are the major sources for RANKL and thus control formation, function and survival of osteoclasts. RANKL is presented to osteoclast precursors by osteocytes in a membrane-bound form through their dendritic processes that can reach beyond the bone surface (Brunetti et al., 2019; Robling and Bonewald, 2020; Xiong et al., 2015).

OPG is a protein that binds RANKL and thereby inhibits RANK-RANKL interactions. By acting as a decoy receptor for RANKL it suppresses osteoclastogenesis and bone resorption. OPG is largely expressed by osteoblasts but again also osteocytes are a main source for this protein (Brunetti et al., 2019).

To conclude, osteocytes can direct osteoclastogenesis and therefore bone resorption either in a positive way by increasing RANKL and decreasing OPG, or in a negative way by reversing the proportions in order to decrease bone resorption (Robling and Bonewald, 2020).

3.3.4. Regulation of osteoblasts

Osteocytes can have direct effects on osteoblasts by secreting a variety of stimulating or inhibiting factors. For example they are able to enhance osteoblastogenesis and thus matrix formation through secretion of lipids like prostaglandin (PGE_2), growth-factors like IGF-1 or glycoproteins like Wnts (Bonewald, 2017). One way of osteocytes to prevent osteoblasts from building bone is by inhibiting the Wnt signaling pathway. Their major sources for antagonizing Wnt-mediated activity in osteoblasts are sclerostin and dickkopf-related protein 1 (DKK1). Anabolic stimuli like mechanical loading, PTH-secretion or PGE_2-secretion on the other hand inhibit sclerostin expression. Sclerostin is a glycoprotein that binds to the low-density lipoprotein receptor-related protein 5 (LRP5) which is a transmembrane protein located on osteoblast membranes and is involved in the canonical Wnt pathway. By binding LRP5, sclerostin inhibits the Wnt signaling pathway and thereby reduces bone formation. On the other hand lower sclerostin levels favor bone formation (Kocijan et al., 2014; Nicol et al., 2018).

3.3.5. Communication with distant organs

As we discussed earlier, osteocytes are connected to blood vessels through their dendritic processes. Since bone is highly vascularized, they are able to secrete factors into the blood

system. Consequently bone is not an inanimate object that solely secures the bodies structure but should additionally be seen as an endocrine organ (Bonewald, 2011). Besides regulating blood calcium levels, osteocytes for example play an important role in regulating the calcium-phosphate household and vitamin D metabolism. By secreting fibroblast growth factor 23 (FGF23) in response to increased calcitriol, calcium or phosphate levels they suppress the expression of the sodium-phosphate cotransporter NPT2 in the proximal tubule in the kidneys. As a result, FGF23 decreases the reabsorption and increases the excretion of phosphate. FGF23 further decreases the activation of calcidiol to calcitriol by inhibiting the expression of 1-α-hydroxylase and subsequently impairs calcium absorption in the gastrointestinal tract (Robling and Bonewald, 2020).

Recent studies also show that bones and muscles communicate with each other beyond mechanical interactions. Especially contracted muscles act as secretory organs targeting bone cells and vice versa bone cells, especially osteocytes, can target muscles. This crosstalk occurs through the secretion of a whole string of soluble factors, some having positive and some negative effects on the opposing tissue. These factors are most likely responsible for the beneficial effects of mechanical loading through exercise or the unfavorable effects of the lack of it. This once again underlines the importance of physical training for bone health (Bonewald, 2019; Bonewald, 2017; Tobias et al., 2014).

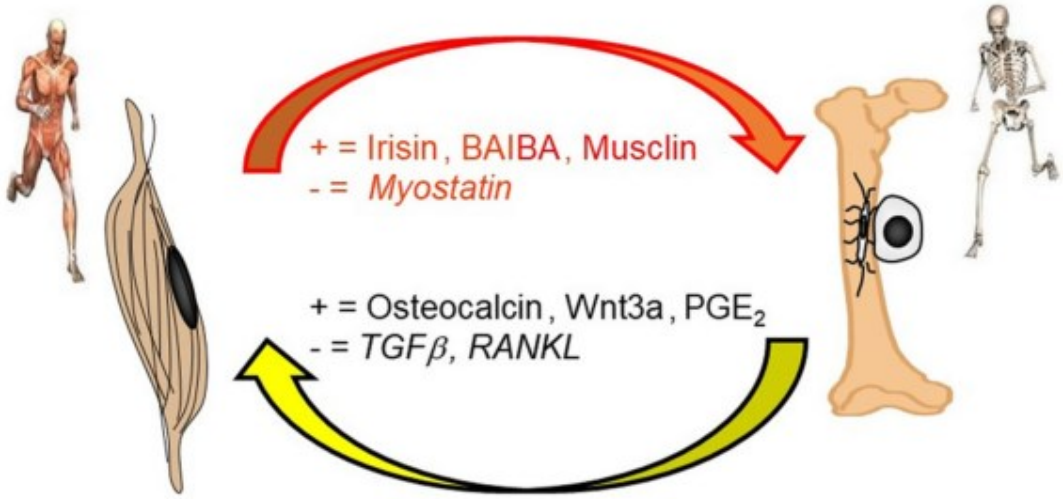

Figure 10: *muscles and bones interact with each other not only on a mechanical level but also by secreting factors that influence each other's metabolism. Especially osteocytes act as endocrine cells targeting for example muscle cells. Bones and muscles can be mechanicaly loaded which triggers the secretion of many of those factors. Mechanical loading occurs for example during physical exercise, which explains beneficial effects of sports (Bonewald, 2019; Tobias et al., 2014).*

3.4. Osteocytes and OI

The role of osteocytes in the development and progression of OI has rarely been investigated so far. As osteocytes are embedded in bone, interactions with their surrounding

matrix are of great importance for them. Today it is still not clear if the impaired collagen structure and the altered bone matrix in OI have an effect on osteocyte function and viability. The altered collagen-to-osteocyte or bone-to-osteocyte interactions might for example have an effect on mechanotransduction and consequently on osteocytic communication with osteoblasts and osteoclasts. At this point more studies investigating these questions are needed in order to reveal the exact role of osteocytes in OI (Pathak et al., 2020).

What we know for sure is that the number of osteocyte lacunae is altered in OI. As mentioned earlier, studies from Blouin et al., Imbert et al. and Jandl et al. were already able to show increased osteocyte density in relative small cohorts of OI patients (Blouin et al., 2017; Imbert et al., 2015; Jandl et al., 2020). We hypothesized that a modified lacunocanalicular network architecture may negatively affect mechano-sensing and thereby contribute to bone fragility. Furthermore, osteocyte-directed metabolic pathways that regulate bone turnover might be altered in OI. Higher bone resorption in OI might for example be due to high levels of RANKL, Sclerostin and DKK1, three factors expressed by osteocytes (Mahr et al., 2021). A connection between osteocyte number and secretion of such factors is still elusive.

The present study provides data from a large cohort of pediatric patients with OI type I and for comparison of healthy children and will thereby deepen our knowledge on osteocyte characteristics in OI.

4. Patients and Methods

4.1. Study Cohort

The study cohort consisted of 19 OI type I patients (male n = 13; female n = 6) with an age range from 2.2 to 14.1 years. In six of them qualitative mutations and in 13 quantitative mutations were responsible for gene alterations. All patients were followed at the Shriners Hospital for Children in Montreal, Canada. The clinical diagnosis of OI-I was based on the Sillence-classification, thus patients were of normal or slightly reduced stature and had little to none bone deformities. They were included in the study after a confirmed mutation in collagen type I by molecular diagnostic studies. Patients were eligible for the study if an iliac bone biopsy sample had been obtained before the start of any osteotropic intervention. All clinical, genetic and histomorphometric data were published previously (Rauch et al., 2000).

The study protocol was approved by the Ethics Committee of the Shriners Hospital for Children. Informed consent was obtained in each instance from the subject and/or a legal guardian as appropriate (Mahr et al., 2021; Rauch et al., 2000).

For comparison I used 24 biopsy samples (male n=15; female n= 9) from the pediatric reference cohort established by Glorieux et al in 2000 (Glorieux et al., 2000). These bone biopsies were obtained during medical interventions for various orthopedic conditions that require corrective surgery. All individuals had normal renal function at the time of biopsy and no evidence of any metabolic bone disorder. None of them received medication known to affect bones prior to the surgery or were immobilized by their condition. Again the study protocol was approved by the Ethics Committee of the Shriners Hospital for Children and informed consent was obtained in each instance from the subject and/or a legal guardian as appropriate (Glorieux et al., 2000; Mahr et al., 2021). For the control group we chose an age range from 2.0 to 14.7 years that did not differ from the OI study population (*p*-value: 0.067, Mann-Whitney U test).

OI group (n=19)		Control group (n=24)	
Biopsy Sample	**Age**	**Biopsy Sample**	**Age**
OI-2	11.0	Ref-3	13.0
OI-3	7.3	Ref-4	13.0
OI-6	7.6	Ref-6	2.0
OI-7	5.4	Ref-9	12.5
OI-8	8.1	Ref-10	2.0
OI-10	4.2	Ref-13	12.0
OI-11	7.6	Ref-15	8.8
OI-12	8.5	Ref-16	14.2
OI-13	3.3	Ref-20	11.7
OI-14	13.0	Ref-22	8.15
OI-15	8.2	Ref-24	14.7
OI-16	4.1	Ref-30	14.6
OI-17	2.3	Ref-33	13.3
OI-18	14.1	Ref-36	3.0
OI-19	2.6	Ref-37	8.7
OI-20	2.2	Ref-40	9.1
OI-21	9.0	Ref-41	10.7
OI-22	8.3	Ref-42	3.3
OI-23	4.2	Ref-43	5.2
		Ref-47	10.9
		Ref-49	10.6
		Ref-59	4.5
		Ref-64	9.4
		Ref-67	2.1

***Table 1**: Left column shows number and age of the OI patients, right column shows number and age of the reference cohort we used as control group. We excluded OI biopsy samples with splice mutations. The age of the study cohort did not differ from the age of the control group (*p-value: 0.067, *Mann-Whitney U test (Mahr et al., 2021).*

4.2. Biopsy sample preparation

I used residual samples blocks prepared originally for bone histomorphometry (Glorieux et al., 2000; Rauch et al., 2000). Briefly biopsies were obtained from a site located 2 cm below and behind the anterior superior iliac spine (Roschger et al., 2008). Ideally complete biopsy cores containing both cortices could be obtained and no side effects other than transient local discomfort due to this procedure were noted. For the next step in preparing the biopsies they were fixed in 10% phosphate-buffered formalin for 48-72h at room temperature. Next, they had to be dehydrated in increasing concentrations of ethanol and cleared with xylene. After that the bone samples were embedded in methylmethacrylate (MMA). Finally, after polymerization, the residual blocks were trimmed with a diamond saw (Glorieux et al., 2000).

For the present study I re-used those residual sample blocks to perform quantitative back-scattered electron microscopy with a high-resolution field emission scanning electron microscope in order to analyze osteocyte lacunae sections (OLS) (Mahr et al., 2021). It should be noted that these samples were already analyzed in 2008 and 2009, by qBEI using a Zeiss DSM 962 digital scanning electron microscope with a lower resolution that did not allow to analyze osteocyte lacunae characteristics (Fratzl-Zelman et al., 2009; Roschger et al., 2008; Roschger et al., 2008).

In order to analyze the samples containing cortical and cancellous bone with the scanning electron microscope, the surfaces of MMA-blocks have to be plane parallel and completely smooth without any kind of scratches. To achieve this, samples were grinded with two different sanding plates and then polished with two different polishing plates. Next the samples have to be fixed on a small plate in order to place them in the scanning electron microscope. For the final step, the surface has to be coated with a thin carbon layer by vacuum evaporation (Roschger et al., 1998; Roschger et al., 2008).

The most important instrument we used for carrying out our experiments was a back-scattered electron microscope. In the following paragraphs I will briefly explain the technology behind such a microscope and the methods we used to obtain our results with it.

4.3. Field Emission Scanning Electron Microscopy (FESEM)

Field emission scanning microscopy (FESEM) is performed with a backscattered electron microscope that produces images of a sample by scanning the surface with a focused beam of electrons. Signals containing information about the surface topography and composition

of the sample are produced by the interaction of electrons with atoms in the sample (Hartmann et al., 2021).

4.4. Quantitative Backscattered Electron Imaging (qBEI)

The basis of the qBEI method, is that the intensity of electrons backscattered from the surface of a bone biopsy is proportional to the concentration of mineral and therefore calcium in the specific area. Digital, grey-level images can be obtained in an approximately 0.5µm thick surface layer of the sample. The fraction of the electrons backscattered increases with the atomic number Z of the atoms hit by the beam. In bone, calcium has the highest atomic number (Z=20) and therefore strongly influences the intensity of the backscattered electrons (BE) (Roschger et al., 1998; Roschger et al., 2008). The electron beam energy is being kept at 20 kV with a working distance of 10mm in the FESEM. BE images were captured from the cortical and cancellous part of the bone at a magnification of x160. A 901 x 676µm wide area was scanned per image and the pixel resolution was 0,9µm/pixel and had a grey-level resolution of 256 grey-level steps.

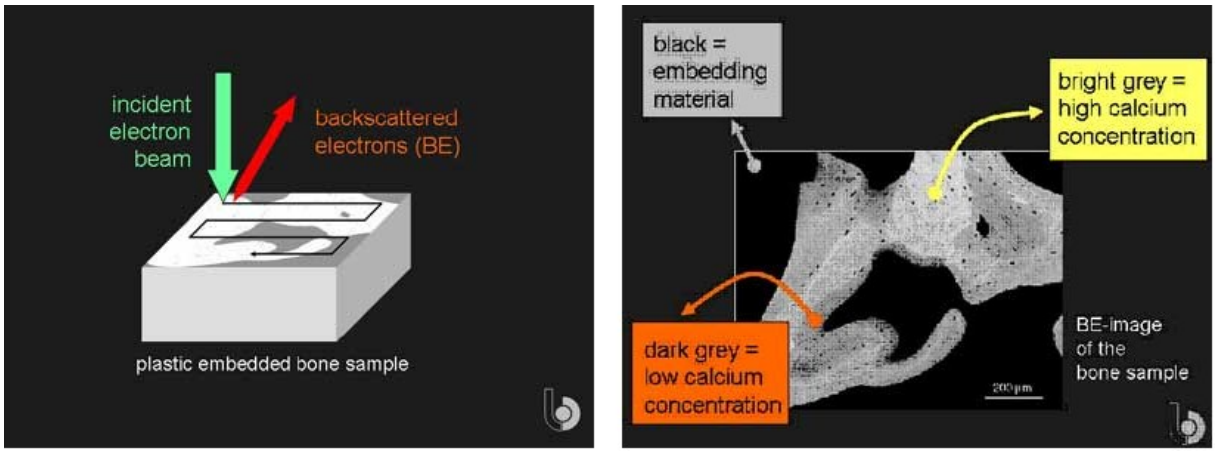

Figure 11: *left picture shows how electrons get backscattered from the polished surface of the MMA embedded bone sample. The intensity of backscattered electrons correlates strongly with the material on the surface of the sample. Right picture shows a typical grey-level image of a bone biopsy sample taken with a scanning electron microscope (SEM). The grey levels correlate with the concentration of calcium in the mineralized matrix (Roschger et al., 1998).*

4.5. Osteocyte Lacunae Section Analyses

The 2D images, obtained by the qBEI method were analyzed to characterize the osteocyte lacunae. An osteocyte lacuna is defined as a 3D cavity within the mineralized bone matrix, occupied by an osteocyte. We cannot be completely sure that every cavity was holding a living osteocyte at the moment of obtaining the biopsy as we are only measuring the lacunae and not the osteocytes itself. So, this technique should be viewed as an indirect measurement of osteocytes. It is not perfect but still the closest and easiest way of counting

osteocytes we know at this moment. By using a custom-made macro in ImageJ software (version 1.50f; NIH, Bethesda, MD, USA; https://imagej.nih.gov/ij/) 2D analysis of osteocyte lacunae sections (OLS) were performed. A minimal bone area of 0.5mm^2 was set to be appropriate for OLS analysis. Further we set a grey-level threshold to discriminate between mineralized bone matrix and OLS area at a fixed grey level of 55 corresponding to a value of 5.2 weight % calcium. To discriminate OLS from either surrounding mineralized bone matrix or from the osteonal channels a size threshold was set between 5 µm^2 and 200 µm^2 (Blouin et al., 2017).

Five parameters were characterized:

(1) OLS-density

- the number of OLS per mineralized bone matrix area (number of OLS/mm^2)

(2) OLS-porosity

- OLS total area / (mineralized bone matrix area + OLS total area) (%)

(3) OLS-area

- mean value of the OLS area per sample (µm^2)

(4) OLS-perimeter

- mean value of the OLS perimeter per sample (µm)

(5) OLS-AR

- mean value of the OLS aspect ratio (AR) per sample
- AR is a measure of elongation to describe the particle's fitted ellipse: (major axis) / (minor axis). A value of 1 indicates a perfect circle and increasing values indicate increasingly elongated shape. AR values >10 were excluded (Blouin et al., 2017).

4.6. Statistical Analysis

We compared OLS parameters in the OI cohort (n=19) and in the control group (n=24) that did not differ significantly in age. Further we compared these parameters with data from OI type V patients published by Blouin et al (Blouin et al., 2017) by using an unpaired T-test. Characteristics of the biopsy samples were described using frequencies and percentages for categorical variables and means and standard deviation (SD) for continuous variables. For variables that did not conform to a normal distribution, medians and interquartile ranges (IQR) were computed. The distribution of each parameter was assessed by normality plots and by Shapiro–Wilk test on a total sample and also on subsamples of OI and healthy children (Mahr et al., 2021).

In order to compare groups (OI type I vs healthy children, OI type I qualitative vs quantitative mutations) we used an independent sample T-test or Mann-Whitney U test for continuous

variables and a Chi-square test for categorical variables. When comparing OLS parameter in trabecular and cortical bone from the same patient we used a paired T-test (Mahr et al., 2021).

Analyses were done in IBM SPSS version 26 (IBM Corp. Released 2019. IBM SPSS Statistics for Windows, Version 26.0. Armonk, NY, USA: IBM Corp) and in GraphPad Prism version 9.1.0 for Windows (GraphPad Software, San Diego, CA, USA, www.graphpad.com accessed on 10th of April 2021) (Mahr et al., 2021).

5. Results

The results we obtained were also published in 2021 in the International Journal of Molecular Science (IJMS) (Mahr et al., 2021). In this study we additionally related osteocyte lacunae characteristics to histomorphometric parameters published previously by Glorieux et al., for healthy controls (Glorieux et al., 2000) and by Rauch et al., for OI (Rauch et al., 2000). Moreover, we provided reference data on bone mineral density distribution for healthy children and children with osteogenesis imperfecta type I obtained with the Field Emission Scanning Electron Microscope. For more information see supplementary material B.

5.1. Increased OLS-density but normal OLS-size in OI type I bone

Figure 13 shows examples of transiliac bone biopsy samples which were analyzed by using quantitative backscattered electron imaging. It further shows qBEI images of cortical and trabecular sections which are used for the characterization of osteocyte lacunae. In the overview images of the biopsy samples a decreased number and thickness of trabeculae and a decreased cortical width can be observed in the OI sample when compared to the healthy bone sample. Furthermore an increased density of osteocyte lacunae in OI bone can especially be seen in the images of the cortical section.

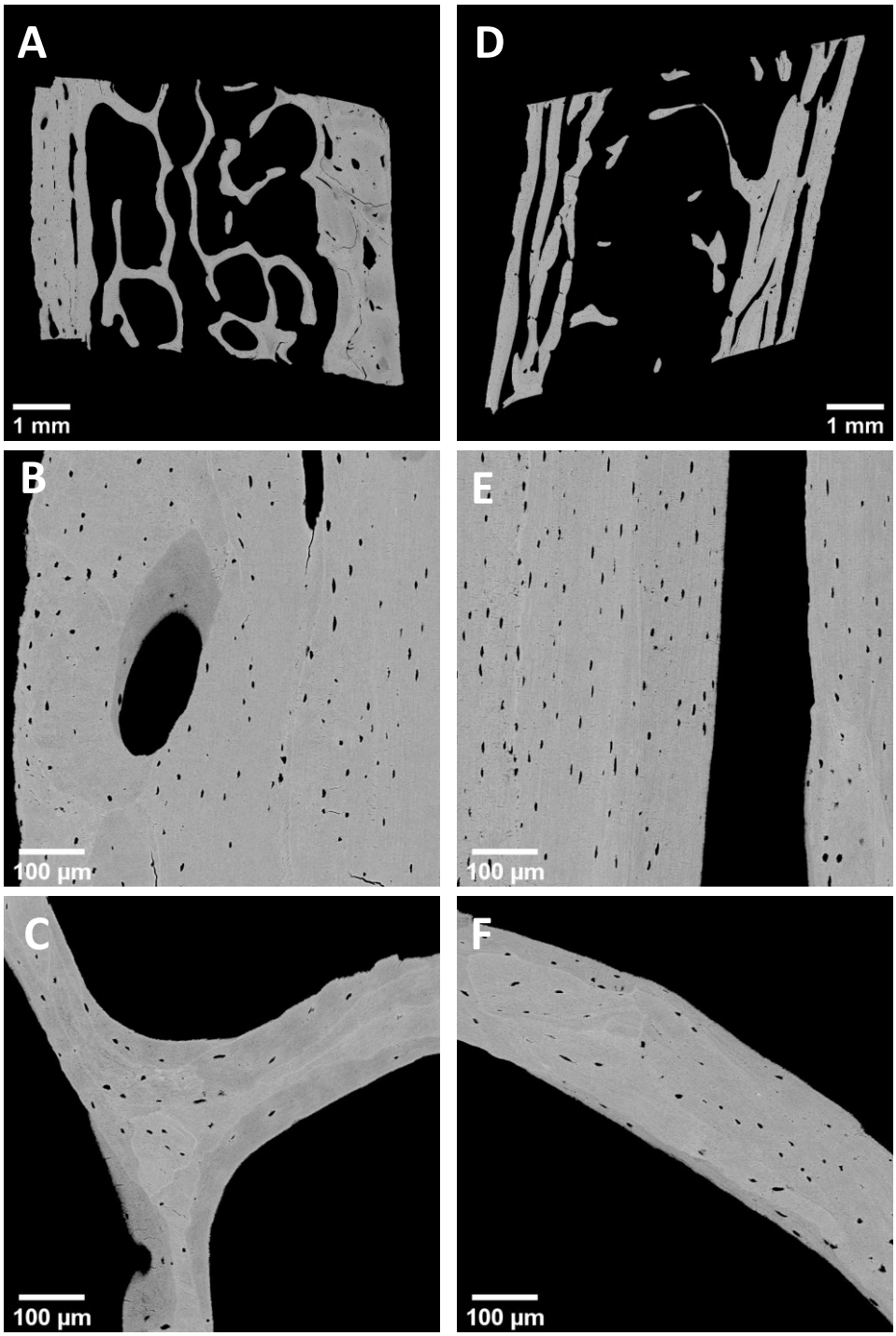

Figure 12: *"Example of quantitative backscattered images of transiliac bone biopsy samples from healthy children (A, B, C) and children with OI type I (D, E, F). Typical backscattered electron images of a complete biopsy samples (A) from a 2-year-old healthy boy and (D) from a 7.6-year-old female OI type I patient with qualitative mutation. Note the decreased number and thickness of trabeculae and the decreased cortical width in OI type I bone. Example of quantitative backscattered images used for OLS-analysis of cortical bone (B, E) and trabecular bone (C, F). Note the increased osteocyte lacunar density that can be judged especially in the cortical compartment of OI type I bone (B versus E). Nominal magnification: A and D: 65x; B, C, E and F: 130x" (Mahr et al., 2021).*

Table 2 shows the results obtained from the OLS analysis in cortical and trabecular bone of OI type I patients in comparison to the control group. Figure 14 shows the data in graphs presented using the box-and-whisker plot.

OLS-density in OI type I bone is increased by +50.66% in cortical bone and +61.73% in trabecular bone versus controls (all $p < 0.001$). OLS-porosity in OI type I bone is increased by +49.15% in cortical bone and +40.73% in trabecular bone when compared to controls (all $p<0.001$). OLS-size (OLS-area and OLS-perimeter) are similar in cortical bone from OI patients and controls. OLS-aspect ratio was also found to be similar in trabecular bone, while in cortical bone OLS-aspect ratio was increased indicating more elongated lacunae in OI type I than in healthy controls (+16.8%, $p<0.003$) (Mahr et al., 2021).

When analyzing OLS parameters from the same patient we observed that OLS-density as well as OLS-porosity are lower in trabecular bone than in cortical bone. This is valid in OI patients (-11.7%, $p<0.0334$; -13.64%, $p<0.0268$), as well as, in controls (-17.7%, $p<0.0001$; -8.45%, $p=0.0014$). OLS-area and OLS-perimeter are similar in trabecular and in cortical bone in both groups. Interestingly, in the OI group OLS-aspect ratio is higher in cortical than in trabecular bone whereas there is no significant alteration in the control group (Mahr et al., 2021).

	Trabecular bone			**Cortical bone**			**Trabecular vs cortical bone**	
	OI type I (n=18)*	**Controls (n=24)**	**p-value**	**OI type I (n=19)**	**Controls (n=24)**	**p-value**	**OI type I (p-value)**	**Controls (p-value)**
OLS-parameters								
OLS-Density (number/mm^2)	365.60 (±67.73)	226.00 (± 26.75)	<0.0001	413.80 (± 86.25)	274.30 (± 60.26)	< 0.0001	0.0334	< 0.0001
OLS-Porosity (%)	0.76 [0.64; 0.81]	0.54 [0.48; 0.60]	<0.0001	0.88 [0.72; 1.06]	0.60 [0.53; 0.69]	< 0.0001	0.0268	0.0014
OLS-Area (µm^2)	21.20 (± 3.16)	23.63 (± 3.01)	0.0150	21.53 (± 3.66)	23.19 (± 3.34)	0.1278	0.5944	0.5211
OLS-Perimeter (µm)	19.65 (± 1.51)	20.42 (± 1.50)	0.1070	20.61 (± 2.21)	20.30 (± 2.09)	0.6368	0.1110	0.7512
OLS-Aspect Ratio	2.63 (± 0.18)	2.55 (± 0.22)	0.2185	2.92 [2.63; 3.27]	2.50 [2.27; 2.72]	0.0003	0.0020	0.2522

Table 2: *Results of OLS analysis of OI type I patients and healthy controls. Values are presented as mean (± standard deviation) or median [interquartile range: 25%; 75%] (Mahr et al., 2021). *In one sample no trabecular bone was present. All other samples contained two cortices and trabecular bone (Mahr et al., 2021).*

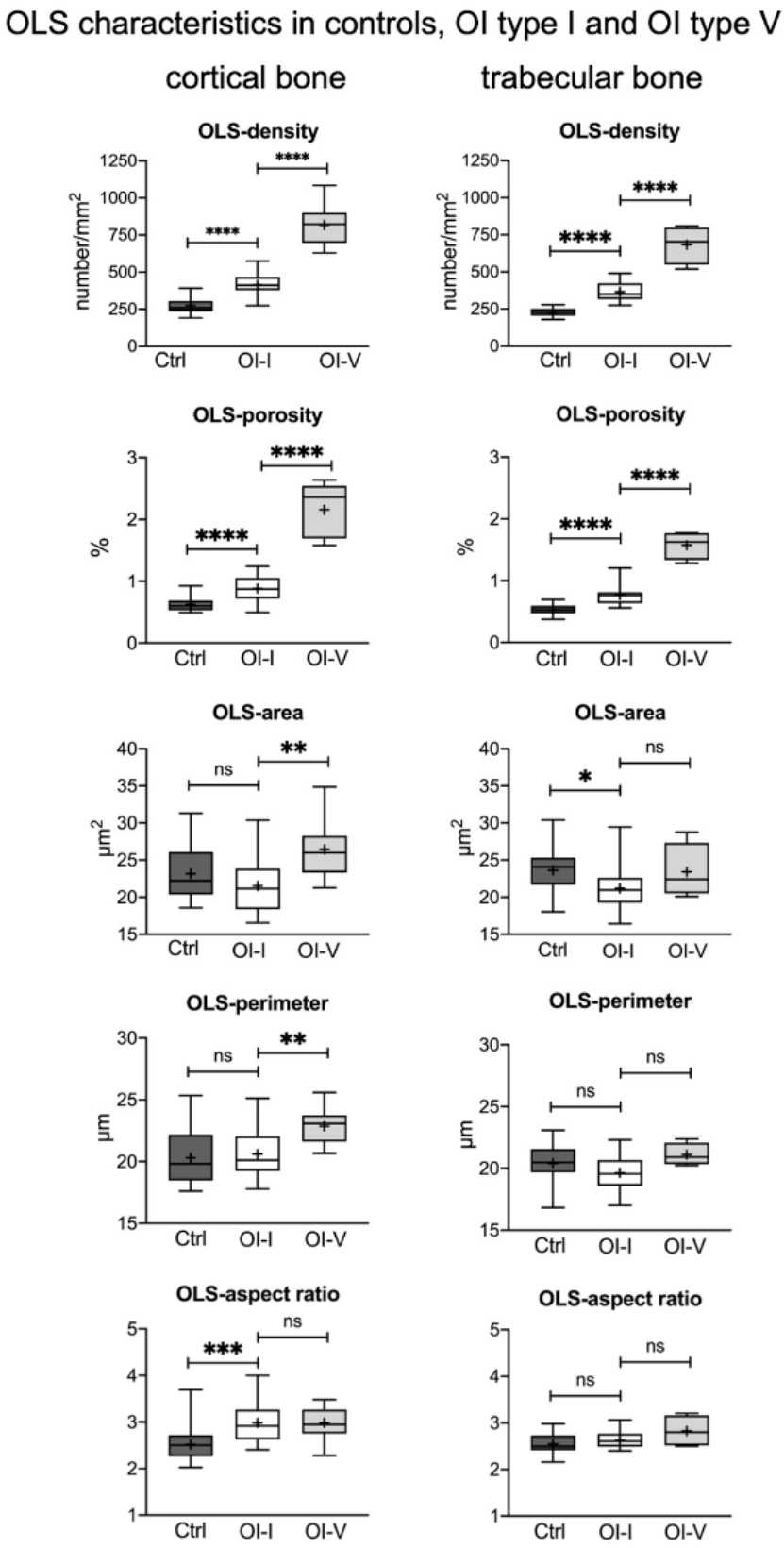

Figure 13: *"Results of OLS analysis: comparison of OLS characteristics in transiliac bone biopsy samples from children with OI type I (n=19) versus controls (n=24) and versus OI type V (n= 15, age: 8.7 ± 4 years-old) previously presented by Blouin et al (Blouin et al., 2017). * p < 0.05, ** p < 0.01, ***p < 0.001, **** p < 0.0001" (Mahr et al., 2021).*
"The left column shows results in trabecular and the right column results in cortical bone. Data is presented using the Box-Whisker-Plot with the horizontal line in the middle showing median values and the top and bottom lines of the boxes showing the interquartile range. The + inside the boxes represents mean values and the horizontal lines above and below the boxes show maxima and minima" (Mahr et al., 2021).

5.2. Correlation of OLS characteristics between trabecular and cortical bone

We observed high positive correlations for OLS-density (r = 0.778, p < 0.0001) and moderate positive correlations for OLS-porosity (r = 0.573, p < 0.0001). We further observed low positive correlations for OLS-area (r = 0.328, p = 0.0338) and OLS-aspect ratio (r = 0.490, p = 0.0001) between trabecular and cortical bone. Graphs presenting the data are shown in Figure 16 (Mahr et al., 2021).

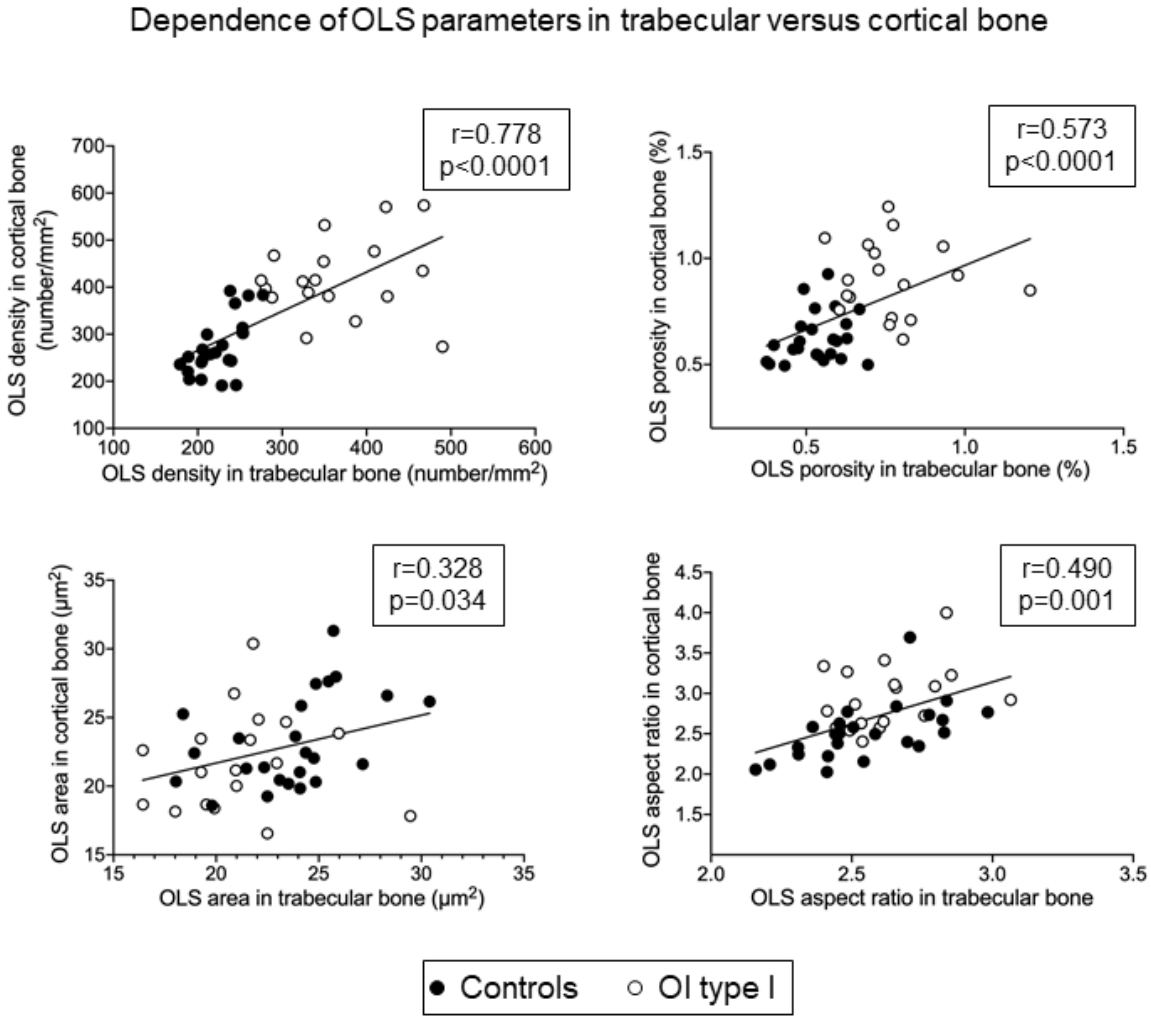

Figure 14: *"Dependency of OLS density (A), OLS porosity (B), OLS area (C) and OLS aspect ratio (D) in trabecular versus cortical bone (total sample analysis). Note that OLS-density and OLS-porosity in OI type I bone (white circles) is always higher than in controls (black circles). In contrast, there is no clear separation between both groups for OLS area and OLS aspect ratio" (Mahr et al., 2021).*

5.3. Differences between Qualitative and Quantitative Mutations

We did not find any statistical differences between OLS characteristics of OI patients with quantitative mutations and qualitative mutation. Only cortical OLS-porosity is significantly higher in qualitative mutations than in quantitative mutations (1.03% ± 0.16 vs 0.81% ± 0.17; p=0.019) (Mahr et al., 2021).

5.4. Comparison of OI type I and OI type V

As mentioned earlier, we further compared the present data with OLS characteristics of OI type V patients presented by Blouin et al in 2017 (Blouin et al., 2017). OI type V bone consists predominantly of primary woven bone with disorganized collagen fibrils (Blouin et al., 2017; Glorieux et al., 2000). OLS-density and OLS-porosity in OI type I bone are about 50% lower in both bone compartments when compared to OI type V bone. Moreover, in OI type V bone OLS-area and OLS-perimeter are significantly larger in cortical bone (+22.8%, p = 0.0012; +10.92%, p = 0.0040) whereas there are no statistical differences of OLS-size in trabecular bone present. Graphs presenting the differences between OI type I and type V are shown in Figure 15 (Mahr et al., 2021).

5.5. Role of Age

Whereas there is no significant relationship between age and OLS parameters in OI type I bone, in the control group OLS-area increases significantly with age in cortical bone (r = 0.437, p = 0.039). When we pooled data from all biopsy samples into one group (thus n = 43), OLS-density decreases significantly with age (r = -0.375, p = 0.042) in trabecular but not in cortical bone. Graphs presenting correlations between OLS-parameters and age are presented in Figure 17 (Mahr et al., 2021).

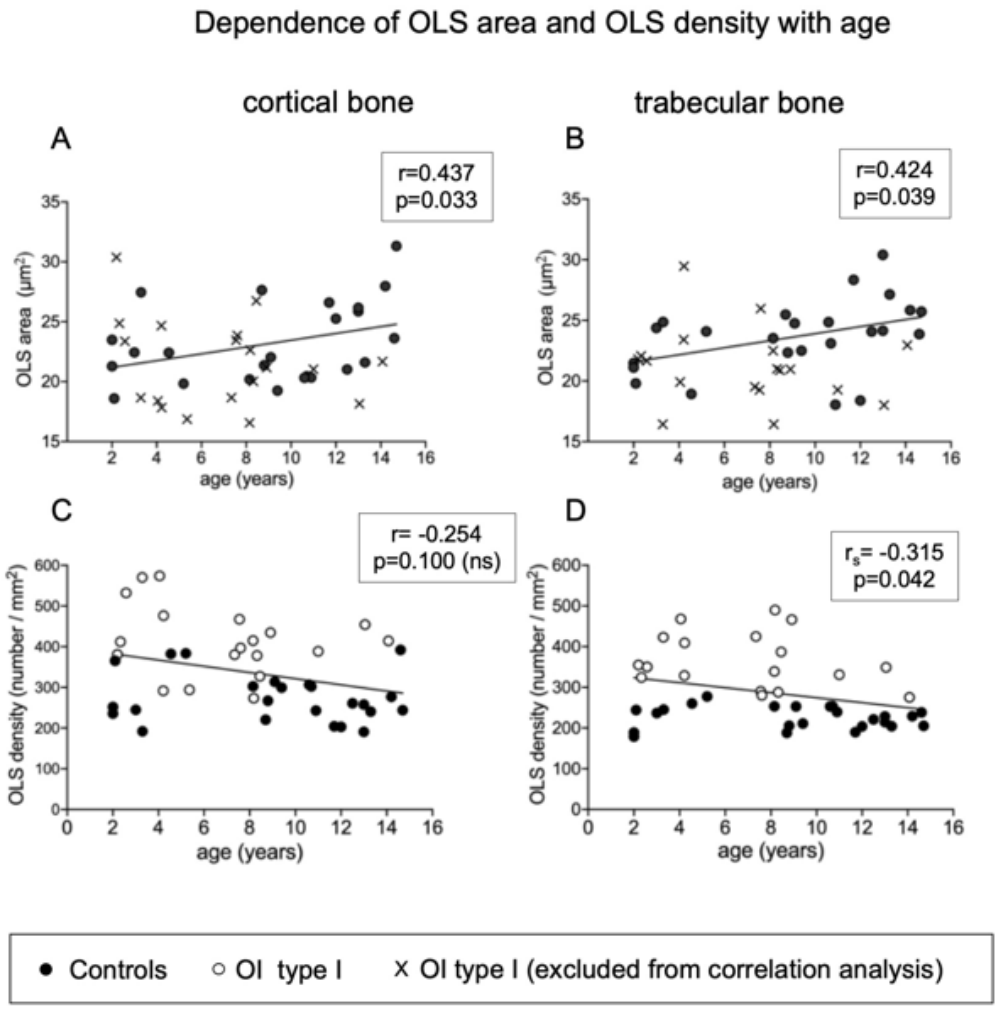

Figure 15: *"Dependency of OLS area **(A, B)** and OLS density **(C, D)** with age. OLS area increases slightly with age in controls but not in OI type I bone (p= 0.308 and 0.463, respectively for cortical and trabecular bone). In contrast, OLS density is negatively correlated with age (total sample analysis). Note that at all ages, OLS density is higher in OI type I (white circles) than in controls (black circles)" (Mahr et al., 2021).*

5.6. Correlations of OLS characteristics and histomorphometric parameters

As mentioned earlier all results were published in 2021 by Mähr et al. in the IJMS where we presented detailed information on the correlation of OLS characteristics with bone histomorphometric parameters (Mahr et al., 2021). Briefly, OLS density and OLS porosity are negatively correlated with structural histomorphometric parameters like cortical width and bone volume / tissue volume. Furthermore, OLS density and OLS porosity are negatively correlated with indices of osteoblast function like mineral apposition rate, bone formation rate / osteoblast surface and osteoid thickness. Finally, we found positive correlations of OLS density and OLS porosity with surface-based bone formation indices like osteoblast surface / bone surface, osteoid surface / bone surface and mineralizing surface / bone surface. Interestingly, correlations of OLS area and OLS perimeter with

histomorphometric parameters were observed in trabecular bone (Mahr et al., 2021). For further information see supplementary material B.

6. Discussion

In the present study we reevaluated bone biopsy samples of a previously presented reference cohort of healthy children and a study cohort of children with OI type I in order to analyze OLS characteristics. The method we applied was developed previously by Blouin et al., in 2017 to analyze OLS characteristics in OI type V bone, a distinct form of OI caused by a gain-of-function mutation in the *IFITM5* gene (Blouin et al., 2017). OI type I represents a classical form of OI with collagen-gene mutations. At the tissue level, OI type I is characterized by hypermineralization of the matrix, increased osteoblast number, osteoclast number, osteoid surface and impaired osteoblast function (Mahr et al., 2021).

In accordance with previous studies of this OI cohort, we almost found no significant differences for OLS-characteristics between quantitative and qualitative mutations (Fratzl-Zelman et al., 2014; Paschalis et al., 2016; Roschger et al., 2008). Only OLS-porosity in cortical bone was modestly increased in patients with qualitative mutations. The observed lack of mutation-specific alterations further indicates that specific collagen defects do not primarily cause the abnormalities in OI bone with collagen-gene mutations. Consequently, we pooled all OI type I samples and analyzed OLS parameters in the total study population (Mahr et al., 2021).

We found several differences in OLS characteristics between OI type I and healthy controls for what reason we can draw following conclusions:

- First, the most striking observation is the increased OLS-density in cortical and trabecular bone of OI patients. Consequently, we can conclude that the total amount of bone matrix surrounding a single osteocyte is reduced in OI type I. This is in accordance with bone histomorphometric study from Rauch et al., showing that although the number of osteoblasts is increased in OI the matrix formed at the single cell level is markedly reduced (Rauch et al., 2000).
- Second, the OLS-aspect ratio is increased in cortical bone of OI patients. When we combine this information with the fact that osteocytes usually align with the collagen direction, this surprisingly suggests the presence of more primary bone in the OI type I cortex as this type of bone is lamellar and seems to be poorly remodeled into osteonal bone (Mahr et al., 2021).

The few published studies that dealt with osteocyte characteristics in OI consistently report an increased number of osteocytes in human OI patients and mouse models (Carriero et

al., 2014; Grabner et al., 2001; Imbert et al., 2015; Jones et al., 1999; Nijhuis et al., 2019; Rauch et al., 2000; Zimmermann et al., 2019). For example, in 2015 Imbert et al., noted a 50% increased osteocyte lacunae density in five children with OI compared to three healthy controls. This observation is in accordance to our data, although, the reported values are much higher in OI patients (640.8 ± 195/mm^2) and in controls (395.8 ± 15.8/mm^2) than in our study. This might be because they obtained the bone samples after corrective surgery from lower extremities and not from the iliac crest. Indeed, in 2019 Zimmermann et al., reported similarly high values in pediatric femoral bone (Zimmermann et al., 2019). Our study is therefore more comparable to the one Jandl et al., performed in 2020 on six children as they also used iliac bone (Jandl et al., 2020). Indeed, the OLS-density we measured in trabecular bone of our healthy reference cohort is very similar to their values. However, the density of the lacunae they found in cortical bone of their healthy controls is twice as high as in our study (537 ± 127 mm^2 vs 274.65 ± 60.14 mm^2). The reason for this discrepancy is most likely that we excluded primary bone areas from our analysis. Primary bone predominately consists of highly porous woven bone and contains significantly more osteocyte lacunae than secondary lamellar bone. It is formed during skeletal growth, as part of a process called modeling drift, where bone apposition and resorption occur on opposite surfaces of the two cortical plates in order to increase the ilium width (Rauch et al., 2006). Normally, primary bone is formed as lamellar sheets that run parallel to the periosteal surface before being remodeled into osteonal bone (Mahr et al., 2021; Parfitt et al., 2000). However, when children are in a phase of growth spurt, loosely organized woven bone is quickly laid down. The collagen I fibrils are arranged randomly and osteocyte density is elevated (Hernandez et al., 2004). Later on, wove bone becomes remodeled into secondary lamellar bone. Another problem in primary bone is that osteocyte lacunae are not clearly distinguishable from unmineralized spaces as the woven bone matrix is highly porous and unorganized. Consequently, the measured lacunae density in those areas might be overestimated. “Woven bone can be distinguished from lamellar bone on qBEI images by the typical increased cellularity and elevated mineralization compared to the adjacent remodeled bone” (Mahr et al., 2021). Figure 17 shows an example of primary woven bone areas.

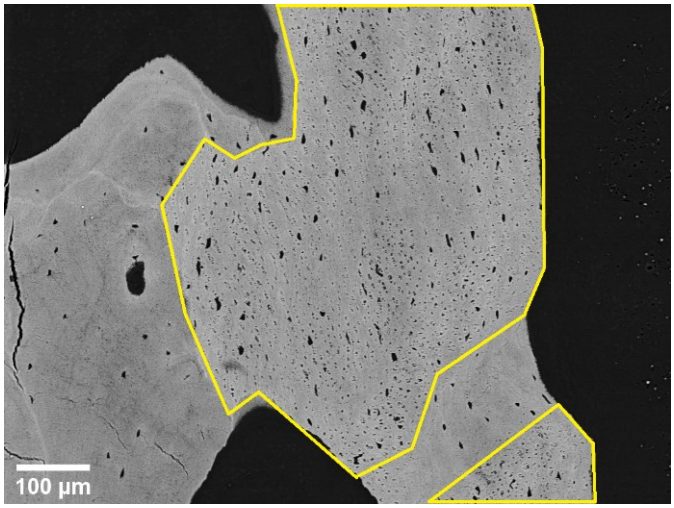

Figure 16: *primary woven bone is marked by yellow lines. The bone tissue is characterized by randomly arranged collagen I fibrils, elevated osteocyte density, increased cellularity, elevated mineralization and highly disorganized bone matrix (Parfitt et al., 2000). These areas were excluded for the analysis of OLS-parameters (Mahr et al., 2021).*

We observed areas with an osteocyte lacunae density of about 500.6 ± 149/mm^2 in half of our control biopsy samples. These children most likely were in a situation of growth spurt at the time of obtaining the biopsy samples. However, the other half of the samples did not show any areas of primary woven bone. Consequently, in order to establish reference data, we decided to exclude all areas of primary woven bone from our analysis. Interestingly no such areas were found in the biopsy samples from our OI study cohort.

Next, I would like to discuss the increased OLS-aspect ratio in the cortices of OI bone. As aspect ratio measures the elongation of osteocyte lacunae, higher values of this parameter indicate a more elongated lacunar shape. Osteocytes usually align their longest axis parallel to the preferred collagen orientation (Repp et al., 2017). Paired with the observed increase in OLS-aspect ratio this fact indicates that the relative amount of parallel lamellar bone in cortical bone of children with OI formed by periosteal apposition is higher than in cortical bone of controls. To put it another way, the remodeling process of primary woven into secondary osteonal bone is delayed or disturbed in OI. This assumption is in line with previous studies (Jones et al., 1999). On the other hand, smaller OLS-aspect ratio values would indicate more secondary remodeled bone in which there is no predominant collagen orientation within the 2D image plane (Mahr et al., 2021).

Concerning the correlations between OLS parameters and histomorphometric parameters especially two observations are worth discussing. First of all, the correlation between increased OLS density and increased surface-based bone formation indices which is in line with previous findings that showed that a reduced matrix production rate of osteoblasts is partially being compensated by an increased number of osteoblasts (Mahr et al., 2021). Again, this is an indication of abnormal osteoblast differentiation. Second, we observed a

positive correlation of OLS-area with osteoid thickness, which we interpret as enhanced osteocytic osteolysis, a possible mechanism to provide additional mineral deposition in the bone matrix. Of note, hypermineralization is a characteristic feature of OI bone.

There are several limitations in our study: We have first to underline that our study solely detects osteocyte lacunae within the mineralized matrix and not living osteocytes. Therefore, we cannot make any statements on the viability of the osteocytes residing in those lacunae. Another limitation is that neither pubertal stages nor serum markers of bone metabolism were evaluated at the time of obtaining the biopsy samples. Although the distribution of the sexes was similar in both groups (62.5% males in controls; 68.4% males in OI group) we also did not investigate any differences between males and females to avoid blurring of the data due to different stages of puberty. Previous studies however, reported that OLS-size and density do not differ between men and women (Hemmatian et al., 2017; Mahr et al., 2021).

The major strength of our study is that we provide new data on osteocyte lacunae characteristics in 19 children with OI type I and 24 controls (Mahr et al., 2021). Thereby we greatly expand the available information on the topic of osteocytes in OI bone as studies up to now were only carried out on very few patients.

7. Conclusion

The aim of this study was to verify previous single observations of alterations concerning osteocyte lacunae characteristics in OI, by analyzing 42 bone transiliac bone biopsy samples from children with OI type I and healthy controls. The here presented study population is up to now the largest cohort of children with OI in which osteocytes have been characterized and therefore the obtained data can be further used as reference values. We can fully confirm that OLS-density and OLS–porosity are significantly elevated in OI type I bone. Due to the elevated number of samples we used, the results we obtained are statistically highly robust (Mahr et al., 2021). Now more studies investigating osteocyte viability, function and network are needed in order to further understand the specific role of osteocytes in the pathology of osteogenesis imperfecta.

8. Supplementary Material

A)

Mähr et al.: Bone properties in Osteogenesis imperfecta: what can we learn from a bone biopsy beyond histology?

Online available at: https://link.springer.com/article/10.1007/s10354-021-00818-w

B)

Mähr et al.: Increased Osteocyte Lacunae Density in the Hypermineralized Bone Matrix of Children with Osteogenesis Imperfecta Type I.

Online available at: https://www.mdpi.com/1422-0067/22/9/4508/htm

8. Abstract

OBJECTIVES: Classical osteogenesis imperfecta (OI) is caused by dominant mutations in type I collagen leading to decreased bone mass and increased bone fragility. OI type I, clinically the mildest form, is caused either by quantitative or qualitative mutations in collagen type I. OI patients show a hypermineralized bone matrix and an increased bone turnover with elevated number of osteoblasts and osteoclasts. To date very few quantitative data is available concerning osteocytes which are the most numerous and most long living type of bone cell. We hypothesize that the osteocyte number is elevated in OI.

METHODS: We compared 2D osteocyte lacunar sections (OLS) in trabecular and cortical area of transiliac bone biopsy samples from children with OI type I (n=19, age-range: 2.2-14.1 years) with age-matched healthy controls (n=24). Calcium concentration images (pixel resolution: 0.9 µm) were obtained by quantitative backscattered electron imaging using a field emission scanning electron microscope. OLS were discriminated from the surrounding mineralized bone matrix and from the osteonal channels by setting a fixed gray level threshold at 55 (5.2 weight % calcium) and a size range from 5µm² and 200µm². We evaluated OLS-density (OLS-number/mm^2), OLS-porosity (%), mean OLS-area (μm^2) and OLS-perimeter (µm).

RESULTS: OLS-density and OLS-porosity were higher in OI than in controls (trabecular bone: +61,73%, +40,74%; cortical bone: +50,66%, +49,15; all $p < 0.0001$). OLS-area in OI was decreased significantly only in trabecular bone (-10.28%, $p = 0.015$). OLS-perimeter was similar in OI and controls. Noteworthy OLS-porosity was always higher in cortical bone than in trabecular bone.

CONCLUSION: Our results show significantly higher numbers of osteocyte lacunae in bones of children with OI type I compared to healthy bones.

9. Zusammenfassung

ZIELE: Osteogensis imperfecta (OI) wird durch Mutationen im Typ I Kollagen hervorgerufen, was zu verminderter Knochenmasse und erhöhter Knochenbrüchigkeit führt. OI Typ I stellt die klinisch mildeste Form dar und wird entweder durch quantitative oder qualitative Mutationen hervorgerufen. OI Patienten weisen weiters eine Hypermineralisation der Knochenmatrix und erhöhte Zahlen an Osteoblasten und Osteoklasten auf. Über den dritten wichtigen Zelltyp, die Osteozyten sind zum jetzigen Zeitpunkt allerding noch sehr wenige quantitative Informationen vorhanden. Osteozyten sind die häufigsten und langlebigsten Knochenzellen. Wir vermuten, dass die Zahl an Osteozyten im OI Knochen erhöht ist.

METHODEN: 2D Osteozytenlakunen (osteocyte lacunae sections, OLS) im trabekulären und kortikalen Knochen von Beckenkammbiopsien von Kindern mit OI Typ I (n=19) wurden mit denen von gesunden Kindern (n=24) verglichen. Mittels quantitativer Rückstreuelektronenmikroskopie mit einem Field Emission Scanning Mikroskop wurden Grauwert-Bilder aufgenommen mittels derer Osteozytenlakunen charakterisiert wurden. Zur Unterscheidung der Lakunen von der mineralisierten Matrix und von Osteonen haben wir mit Graulevelwerten von bis zu 55 (5,2 Gewichtsprozent Kalzium) und einen Größenbereich von 5µm^2 bis 200µm^2 gearbeitet. Analysiert wurden Dichte (OLS-density; OLS-number/mm^2), Porosität (OLS-porosity, %), Fläche (mean OLS-area, µm^2) und Umfang (OLS-perimeter, µm).

ERGEBNISSE: Dichte und Porosität sind im OI Knochen signifikant höher als bei den Kontrollen (trabekulärer Knochen: +61,73%, +40,74%; kortikaler Knochen: +50,66%, +49,15; all $p < 0.0001$). Die Fläche (OLS-area) ist nur im trabekulären Knochen signifikant vermindert (-10.28%, $p = 0.015$). Der Umfang der Lakunen ist vergleichbar zwischen den beiden Gruppen. Hervorzuheben ist auch, dass die Porosität im kortikalen Knochen höher als im trabekulären Knochen ist.

FAZIT: Unsere Resultat zeigen eine signifikant erhöhte Zahl an Osteozytenlakunen im Knochen von Kindern mit OI Typ I im Vergleich zu den Kontrollen.

I have made every effort to locate all owners of the image rights and have obtained their permission to use the images in this work. Should a copyright infringement nevertheless become known, I request you contact me.

8. Bibliography

Arponen H, Makitie O, Waltimo-Siren J. 2014. Association between joint hypermobility, scoliosis, and cranial base anomalies in paediatric Osteogenesis imperfecta patients: a retrospective cross-sectional study. *BMC Musculoskelet Disord*, 15, 428. https://doi.org/10.1186/1471-2474-15-428

Ayoubi M, van Tol AF, Weinkamer R, Roschger P, Brugger PC, Berzlanovich A, et al. 2021. 3D Interrelationship between Osteocyte Network and Forming Mineral during Human Bone Remodeling. *Adv Healthc Mater*, 10(12), e2100113. https://doi.org/10.1002/adhm.202100113

Bartl R. Struktur und Architektur des Skeletts. Klinische Osteologie. Stuttgart: Georg Thieme Verlag KG; 2014.

Baum J, Brodsky B. 1999. Folding of peptide models of collagen and misfolding in disease. *Curr Opin Struct Biol*, 9(1), 122-128. https://doi.org/10.1016/s0959-440x(99)80016-5

Bella J. 2016. Collagen structure: new tricks from a very old dog. *Biochem J*, 473(8), 1001-1025. https://doi.org/10.1042/BJ20151169

Blouin S, Fratzl-Zelman N, Glorieux FH, Roschger P, Klaushofer K, Marini JC, et al. 2017. Hypermineralization and High Osteocyte Lacunar Density in Osteogenesis Imperfecta Type V Bone Indicate Exuberant Primary Bone Formation. *J Bone Miner Res*, 32(9), 1884-1892. https://doi.org/10.1002/jbmr.3180

Bonewald L. 2019. Use it or lose it to age: A review of bone and muscle communication. *Bone*, 120, 212-218. https://doi.org/10.1016/j.bone.2018.11.002

Bonewald LF. 2011. The amazing osteocyte. *J Bone Miner Res*, 26(2), 229-238. https://doi.org/10.1002/jbmr.320

Bonewald LF. 2017. The Role of the Osteocyte in Bone and Nonbone Disease. *Endocrinol Metab Clin North Am*, 46(1), 1-18. https://doi.org/10.1016/j.ecl.2016.09.003

Boyde A, Travers R, Glorieux FH, Jones SJ. 1999. The mineralization density of iliac crest bone from children with osteogenesis imperfecta. *Calcif Tissue Int*, 64(3), 185-190. https://doi.org/10.1007/s002239900600

Brunetti G, D'Amato G, Chiarito M, Tullo A, Colaianni G, Colucci S, et al. 2019. An update on the role of RANKL-RANK/osteoprotegerin and WNT-ss-catenin signaling pathways in pediatric diseases. *World J Pediatr*, 15(1), 4-11. https://doi.org/10.1007/s12519-018-0198-7

Buenzli PR, Lerebours C, Roschger A, Roschger P, Weinkamer R. 2018. Late stages of mineralization and their signature on the bone mineral density distribution. *Connect Tissue Res*, 59(sup1), 74-80. https://doi.org/10.1080/03008207.2018.1424149

Buenzli PR, Sims NA. 2015. Quantifying the osteocyte network in the human skeleton. *Bone*, 75, 144-150. https://doi.org/10.1016/j.bone.2015.02.016

Byers PH. 2002. Killing the messenger: new insights into nonsense-mediated mRNA decay. *J Clin Invest*, 109(1), 3-6. https://doi.org/10.1172/JCI14841

Carriero A, Doube M, Vogt M, Busse B, Zustin J, Levchuk A, et al. 2014. Altered lacunar and vascular porosity in osteogenesis imperfecta mouse bone as revealed by synchrotron tomography contributes to bone fragility. *Bone*, 61, 116-124. https://doi.org/10.1016/j.bone.2013.12.020

Chen X, Wang L, Zhao K, Wang H. 2018. Osteocytogenesis: Roles of Physicochemical Factors, Collagen Cleavage, and Exogenous Molecules. *Tissue Eng Part B Rev*, 24(3), 215-225. https://doi.org/10.1089/ten.teb.2017.0378

Dallas SL, Bonewald LF. 2010. Dynamics of the transition from osteoblast to osteocyte. *Ann N Y Acad Sci*, 1192, 437-443. https://doi.org/10.1111/j.1749-6632.2009.05246.x

Forlino A, Marini JC. 2016. Osteogenesis imperfecta. *Lancet*, 387(10028), 1657-1671. https://doi.org/10.1016/S0140-6736(15)00728-X

Franz-Odendaal TA, Hall BK, Witten PE. 2006. Buried alive: how osteoblasts become osteocytes. *Dev Dyn*, 235(1), 176-190. https://doi.org/10.1002/dvdy.20603

Fratzl-Zelman N, Misof BM, Roschger P, Klaushofer K. 2015. Classification of osteogenesis imperfecta. *Wien Med Wochenschr*, 165(13-14), 264-270. https://doi.org/10.1007/s10354-015-0368-3

Fratzl-Zelman N, Roschger P, Misof BM, Pfeffer S, Glorieux FH, Klaushofer K, et al. 2009. Normative data on mineralization density distribution in iliac bone biopsies of children, adolescents and young adults. *Bone*, 44(6), 1043-1048. https://doi.org/10.1016/j.bone.2009.02.021

Fratzl-Zelman N, Schmidt I, Roschger P, Glorieux FH, Klaushofer K, Fratzl P, et al. 2014. Mineral particle size in children with osteogenesis imperfecta type I is not increased independently of specific collagen mutations. *Bone*, 60, 122-128. https://doi.org/10.1016/j.bone.2013.11.023

Glorieux FH, Rauch F, Plotkin H, Ward L, Travers R, Roughley P, et al. 2000. Type V osteogenesis imperfecta: a new form of brittle bone disease. *J Bone Miner Res*, 15(9), 1650-1658. https://doi.org/10.1359/jbmr.2000.15.9.1650

Glorieux FH, Travers R, Taylor A, Bowen JR, Rauch F, Norman M, et al. 2000. Normative data for iliac bone histomorphometry in growing children. *Bone*, 26(2), 103-109. https://doi.org/S8756-3282(99)00257-4 [pii]

Glorieux FH, Ward LM, Rauch F, Lalic L, Roughley PJ, Travers R. 2002. Osteogenesis imperfecta type VI: a form of brittle bone disease with a mineralization defect. *J Bone Miner Res*, 17(1), 30-38. https://doi.org/10.1359/jbmr.2002.17.1.30

Grabner B, Landis WJ, Roschger P, Rinnerthaler S, Peterlik H, Klaushofer K, et al. 2001. Age- and genotype-dependence of bone material properties in the osteogenesis imperfecta murine model (oim). *Bone*, 29(5), 453-457. https://doi.org/10.1016/s8756-3282(01)00594-4

Graff K, Syczewska M. 2017. Developmental charts for children with osteogenesis imperfecta, type I (body height, body weight and BMI). *Eur J Pediatr*, 176(3), 311-316. https://doi.org/10.1007/s00431-016-2839-y

Hartmann MA, Blouin S, Misof BM, Fratzl-Zelman N, Roschger P, Berzlanovich A, et al. 2021. Quantitative Backscattered Electron Imaging of Bone Using a Thermionic or a Field Emission Electron Source. *Calcif Tissue Int*, 109(2), 190-202. https://doi.org/10.1007/s00223-021-00832-5

Hemmatian H, Bakker AD, Klein-Nulend J, van Lenthe GH. 2017. Aging, Osteocytes, and Mechanotransduction. *Curr Osteoporos Rep*, 15(5), 401-411. https://doi.org/10.1007/s11914-017-0402-z

Hernandez CJ, Majeska RJ, Schaffler MB. 2004. Osteocyte density in woven bone. *Bone*, 35(5), 1095-1099. https://doi.org/10.1016/j.bone.2004.07.002

Holmbeck K, Bianco P, Pidoux I, Inoue S, Billinghurst RC, Wu W, et al. 2005. The metalloproteinase MT1-MMP is required for normal development and maintenance of osteocyte processes in bone. *J Cell Sci*, 118(Pt 1), 147-156. https://doi.org/10.1242/jcs.01581

Imbert L, Auregan JC, Pernelle K, Hoc T. 2015. Microstructure and compressive mechanical properties of cortical bone in children with osteogenesis imperfecta treated with bisphosphonates compared with healthy children. *J Mech Behav Biomed Mater*, 46, 261-270. https://doi.org/10.1016/j.jmbbm.2014.12.020

Jahn K, Kelkar S, Zhao H, Xie Y, Tiede-Lewis LM, Dusevich V, et al. 2017. Osteocytes Acidify Their Microenvironment in Response to PTHrP In Vitro and in Lactating Mice In Vivo. *J Bone Miner Res*, 32(8), 1761-1772. https://doi.org/10.1002/jbmr.3167

Jandl NM, von Kroge S, Sturznickel J, Baranowsky A, Stockhausen KE, Mushumba H, et al. 2020. Large osteocyte lacunae in iliac crest infantile bone are not associated with impaired mineral distribution or signs of osteocytic osteolysis. *Bone*, 135, 115324. https://doi.org/10.1016/j.bone.2020.115324

Jones SJ, Glorieux FH, Travers R, Boyde A. 1999. The microscopic structure of bone in normal children and patients with osteogenesis imperfecta: a survey using backscattered electron imaging. *Calcif Tissue Int*, 64(1), 8-17. https://doi.org/10.1007/s002239900571

Jovanovic M, Guterman-Ram G, Marini JC. 2021. Osteogenesis Imperfecta: Mechanisms and signaling pathways connecting classical and rare OI types. *Endocr Rev*, https://doi.org/10.1210/endrev/bnab017

Knothe Tate ML, Adamson JR, Tami AE, Bauer TW. 2004. The osteocyte. *Int J Biochem Cell Biol*, 36(1), 1-8. https://doi.org/10.1016/s1357-2725(03)00241-3

Kocijan R, Muschitz C, Fahrleitner-Pammer A, Amrein K, Pietschmann P, Haschka J, et al. 2014. Serum sclerostin levels are decreased in adult patients with different types of osteogenesis imperfecta. *J Clin Endocrinol Metab*, 99(2), E311-319. https://doi.org/10.1210/jc.2013-2244

Mahr M, Blouin S, Behanova M, Misof BM, Glorieux FH, Zwerina J, et al. 2021. Increased Osteocyte Lacunae Density in the Hypermineralized Bone Matrix of Children with Osteogenesis Imperfecta Type I. *Int J Mol Sci*, 22(9), https://doi.org/10.3390/ijms22094508

Mahr M, Blouin S, Misof BM, Paschalis EP, Hartmann MA, Zwerina J, et al. 2021. Bone properties in osteogenesis imperfecta: what can we learn from a bone biopsy beyond histology? *Wien Med Wochenschr*, 171(5-6), 111-119. https://doi.org/10.1007/s10354-021-00818-w

Malhotra V, Erlmann P. 2015. The pathway of collagen secretion. *Annu Rev Cell Dev Biol*, 31, 109-124. https://doi.org/10.1146/annurev-cellbio-100913-013002

Marini JC, Forlino A, Bachinger HP, Bishop NJ, Byers PH, Paepe A, et al. 2017. Osteogenesis imperfecta. *Nat Rev Dis Primers*, 3, 17052. https://doi.org/10.1038/nrdp.2017.52

Marr C, Seasman A, Bishop N. 2017. Managing the patient with osteogenesis imperfecta: a multidisciplinary approach. *J Multidiscip Healthc*, 10, 145-155. https://doi.org/10.2147/JMDH.S113483

Milovanovic P, Zimmermann EA, Riedel C, vom Scheidt A, Herzog L, Krause M, et al. 2015. Multi-level characterization of human femoral cortices and their underlying osteocyte network reveal trends in quality of young, aged, osteoporotic and antiresorptive-treated bone. *Biomaterials*, 45, 46-55. https://doi.org/10.1016/j.biomaterials.2014.12.024

Mueller B, Engelbert R, Baratta-Ziska F, Bartels B, Blanc N, Brizola E, et al. 2018. Consensus statement on physical rehabilitation in children and adolescents with osteogenesis imperfecta. *Orphanet J Rare Dis*, 13(1), 158. https://doi.org/10.1186/s13023-018-0905-4

Nicol L, Wang Y, Smith R, Sloan J, Nagamani SC, Shapiro J, et al. 2018. Serum Sclerostin Levels in Adults With Osteogenesis Imperfecta: Comparison With Normal Individuals and Response to Teriparatide Therapy. *J Bone Miner Res*, 33(2), 307-315. https://doi.org/10.1002/jbmr.3312

Nijhuis WH, Eastwood DM, Allgrove J, Hvid I, Weinans HH, Bank RA, et al. 2019. Current concepts in osteogenesis imperfecta: bone structure, biomechanics and medical management. *J Child Orthop*, 13(1), 1-11. https://doi.org/10.1302/1863-2548.13.180190

Parfitt AM, Travers R, Rauch F, Glorieux FH. 2000. Structural and cellular changes during bone growth in healthy children. *Bone*, 27(4), 487-494. https://doi.org/10.1016/s8756-3282(00)00353-7

Paschalis EP, Gamsjaeger S, Fratzl-Zelman N, Roschger P, Masic A, Brozek W, et al. 2016. Evidence for a Role for Nanoporosity and Pyridinoline Content in Human Mild Osteogenesis Imperfecta. *J Bone Miner Res*, 31(5), 1050-1059. https://doi.org/10.1002/jbmr.2780

Pathak JL, Bravenboer N, Klein-Nulend J. 2020. The Osteocyte as the New Discovery of Therapeutic Options in Rare Bone Diseases. *Front Endocrinol (Lausanne)*, 11, 405. https://doi.org/10.3389/fendo.2020.00405

Qin L, Liu W, Cao H, Xiao G. 2020. Molecular mechanosensors in osteocytes. *Bone Res*, 8, 23. https://doi.org/10.1038/s41413-020-0099-y

Qing H, Ardeshirpour L, Pajevic PD, Dusevich V, Jahn K, Kato S, et al. 2012. Demonstration of osteocytic perilacunar/canalicular remodeling in mice during lactation. *J Bone Miner Res*, 27(5), 1018-1029. https://doi.org/10.1002/jbmr.1567

Rauch F. 2006. Watching bone cells at work: what we can see from bone biopsies. *Pediatr Nephrol*, 21(4), 457-462. https://doi.org/10.1007/s00467-006-0025-6

Rauch F, Glorieux FH. 2004. Osteogenesis imperfecta. *Lancet*, 363(9418), 1377-1385. https://doi.org/10.1016/S0140-6736(04)16051-0

S0140-6736(04)16051-0 [pii]

Rauch F, Travers R, Glorieux FH. 2006. Cellular activity on the seven surfaces of iliac bone: a histomorphometric study in children and adolescents. *J Bone Miner Res*, 21(4), 513-519. https://doi.org/10.1359/jbmr.060108

Rauch F, Travers R, Parfitt AM, Glorieux FH. 2000. Static and dynamic bone histomorphometry in children with osteogenesis imperfecta. *Bone*, 26(6), 581-589. https://doi.org/10.1016/s8756-3282(00)00269-6

Repp F, Kollmannsberger P, Roschger A, Berzlanovich A, Gruber GM, Roschger P, et al. 2017. Coalignment of osteocyte canaliculi and collagen fibers in human osteonal bone. *J Struct Biol*, 199(3), 177-186. https://doi.org/10.1016/j.jsb.2017.07.004

Ricard-Blum S. 2011. The collagen family. *Cold Spring Harb Perspect Biol*, 3(1), a004978. https://doi.org/10.1101/cshperspect.a004978

Robin M, Almeida C, Azais T, Haye B, Illoul C, Lesieur J, et al. 2016. Involvement of 3D osteoblast migration and bone apatite during in vitro early osteocytogenesis. *Bone*, 88, 146-156. https://doi.org/10.1016/j.bone.2016.04.031

Robling AG, Bonewald LF. 2020. The Osteocyte: New Insights. *Annu Rev Physiol*, 82, 485-506. https://doi.org/10.1146/annurev-physiol-021119-034332

Roschger A, Roschger P, Wagermaier W, Chen J, van Tol AF, Repp F, et al. 2019. The contribution of the pericanalicular matrix to mineral content in human osteonal bone. *Bone*, 123, 76-85. https://doi.org/10.1016/j.bone.2019.03.018

Roschger P, Fratzl-Zelman N, Misof BM, Glorieux FH, Klaushofer K, Rauch F. 2008. Evidence that abnormal high bone mineralization in growing children with osteogenesis imperfecta is not associated with specific collagen mutations. *Calcif Tissue Int*, 82(4), 263-270. https://doi.org/10.1007/s00223-008-9113-x

Roschger P, Fratzl P, Eschberger J, Klaushofer K. 1998. Validation of quantitative backscattered electron imaging for the measurement of mineral density distribution in human bone biopsies. *Bone*, 23(4), 319-326.

Roschger P, Paschalis EP, Fratzl P, Klaushofer K. 2008. Bone mineralization density distribution in health and disease. *Bone*, 42(3), 456-466. https://doi.org/10.1016/j.bone.2007.10.021

Schulze E, Witt M, Kasper M, Lowik CW, Funk RH. 1999. Immunohistochemical investigations on the differentiation marker protein E11 in rat calvaria, calvaria cell culture and the osteoblastic cell line ROS 17/2.8. *Histochem Cell Biol*, 111(1), 61-69. https://doi.org/10.1007/s004180050334

Staines KA, Javaheri B, Hohenstein P, Fleming R, Ikpegbu E, Unger E, et al. 2017. Hypomorphic conditional deletion of E11/Podoplanin reveals a role in osteocyte dendrite elongation. *J Cell Physiol*, 232(11), 3006-3019. https://doi.org/10.1002/jcp.25999

Tauer JT, Boraschi-Diaz I, Al Rifai O, Rauch F, Ferron M, Komarova SV. 2021. Male but not female mice with severe osteogenesis imperfecta are partially protected from high-fat diet-induced obesity. *Mol Genet Metab*, 133(2), 211-221. https://doi.org/10.1016/j.ymgme.2021.03.014

Tobias JH, Gould V, Brunton L, Deere K, Rittweger J, Lipperts M, et al. 2014. Physical Activity and Bone: May the Force be with You. *Front Endocrinol (Lausanne)*, 5, 20. https://doi.org/10.3389/fendo.2014.00020

Tsourdi E, Jahn K, Rauner M, Busse B, Bonewald LF. 2018. Physiological and pathological osteocytic osteolysis. *J Musculoskelet Neuronal Interact*, 18(3), 292-303.

van Dijk FS, Cobben JM, Kariminejad A, Maugeri A, Nikkels PG, van Rijn RR, et al. 2011. Osteogenesis Imperfecta: A Review with Clinical Examples. *Mol Syndromol*, 2(1), 1-20. https://doi.org/10.1159/000332228

Van Dijk FS, Sillence DO. 2014. Osteogenesis imperfecta: clinical diagnosis, nomenclature and severity assessment. *Am J Med Genet A*, 164A(6), 1470-1481. https://doi.org/10.1002/ajmg.a.36545

Veilleux LN, Lemay M, Pouliot-Laforte A, Cheung MS, Glorieux FH, Rauch F. 2014. Muscle anatomy and dynamic muscle function in osteogenesis imperfecta type I. *J Clin Endocrinol Metab*, 99(2), E356-362. https://doi.org/10.1210/jc.2013-3209

Vetter U, Fisher LW, Mintz KP, Kopp JB, Tuross N, Termine JD, et al. 1991. Osteogenesis imperfecta: changes in noncollagenous proteins in bone. *J Bone Miner Res*, 6(5), 501-505. https://doi.org/10.1002/jbmr.5650060512

Viguet-Carrin S, Garnero P, Delmas PD. 2006. The role of collagen in bone strength. *Osteoporos Int*, 17(3), 319-336.

Wagermaier W, Klaushofer K, Fratzl P. 2015. Fragility of Bone Material Controlled by Internal Interfaces. *Calcif Tissue Int*, 97(3), 201-212. https://doi.org/10.1007/s00223-015-9978-4

Wang Z, McCauley LK. 2011. Osteoclasts and odontoclasts: signaling pathways to development and disease. *Oral Dis*, 17(2), 129-142. https://doi.org/10.1111/j.1601-0825.2010.01718.x

Ward LM, Rauch F, Travers R, Chabot G, Azouz EM, Lalic L, et al. 2002. Osteogenesis imperfecta type VII: an autosomal recessive form of brittle bone disease. *Bone*, 31(1), 12-18. https://doi.org/S8756328202007901 [pii]

Weber M, Roschger P, Fratzl-Zelman N, Schoberl T, Rauch F, Glorieux FH, et al. 2006. Pamidronate does not adversely affect bone intrinsic material properties in children with osteogenesis imperfecta. *Bone*, 39(3), 616-622. https://doi.org/10.1016/j.bone.2006.02.071

Xiong J, Piemontese M, Onal M, Campbell J, Goellner JJ, Dusevich V, et al. 2015. Osteocytes, not Osteoblasts or Lining Cells, are the Main Source of the RANKL Required for Osteoclast Formation in Remodeling Bone. *PLoS One*, 10(9), e0138189. https://doi.org/10.1371/journal.pone.0138189

Zhang K, Barragan-Adjemian C, Ye L, Kotha S, Dallas M, Lu Y, et al. 2006. E11/gp38 selective expression in osteocytes: regulation by mechanical strain and role in dendrite elongation. *Mol Cell Biol*, 26(12), 4539-4552. https://doi.org/10.1128/MCB.02120-05

Zimmerman SM, Dimori M, Heard-Lipsmeyer ME, Morello R. 2019. The Osteocyte Transcriptome Is Extensively Dysregulated in Mouse Models of Osteogenesis Imperfecta. *JBMR Plus*, 3(7), e10171. https://doi.org/10.1002/jbm4.10171

Zimmermann EA, Riedel C, Schmidt FN, Stockhausen KE, Chushkin Y, Schaible E, et al. 2019. Mechanical Competence and Bone Quality Develop During Skeletal Growth. *J Bone Miner Res*, 34(8), 1461-1472. https://doi.org/10.1002/jbmr.3730